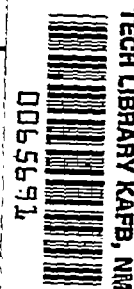


8835
NACA TN 2442



NATIONAL ADVISORY COMMITTEE FOR AERONAUTICS

TECHNICAL NOTE 2442

A PHOTOELASTIC INVESTIGATION OF STRESS CONCENTRATIONS
DUE TO SMALL FILLETS AND GROOVES IN TENSION

By M. M. Frocht

Illinois Institute of Technology



Washington

August 1951

AFMDC
TECHNICAL LIBRARY
AFL 2811



NATIONAL ADVISORY COMMITTEE FOR AERONAUTICS

TECHNICAL NOTE 2442

A PHOTOELASTIC INVESTIGATION OF STRESS CONCENTRATIONS

DUE TO SMALL FILLETS AND GROOVES IN TENSION

By M. M. Frocht

SUMMARY

Factors of stress concentration for deep, sharp, and symmetrically arranged grooves and fillets in tension members have been determined photoelastically and are given in this report. Curves are given showing the distribution of the principal stresses on the section through the grooves. Complete isopachic patterns for several basic cases of grooved bars are included.

INTRODUCTION

Airplane design has always shown a consistent trend toward higher speeds, larger sizes, and higher wing loadings. All these trends tend to make the fatigue problem more important in relation to the static strength problem. This tendency is aggravated by improved methods of static stress analysis, which permit better utilization of material, and by the introduction of materials that have higher static strength without correspondingly increased fatigue strength. Because of these trends, the fatigue problem is now receiving considerable attention.

As part of the current NACA program in this field, the fatigue properties of several widely used airframe materials are being determined. For this purpose it was desired to design some standardized fatigue specimens with stress-concentration factors of known magnitude. Holes, grooves, and fillets are widely used for this purpose because they represent, to some extent at least, practical cases of stress concentration. It was found, however, that there was insufficient information available on the stress concentrations produced by grooves and fillets to cover the range that was considered important. Photoelastic investigations were therefore initiated in order to provide the necessary information.

The specific purpose of the present investigation was to obtain factors of stress concentration for grooves and fillets in bars in tension, as well as distributions of principal stresses along the section

of symmetry through the grooves for values of r/d from 0.011 to 0.08, approximately, for $D/d = 1.5$ and $D/d = 2.0$.

The results obtained are limited to the elastic range. Also, the state of stress in the bars is assumed to be essentially two-dimensional.

The stresses in the uniform parts of the bar, away from the cross section through the discontinuities, were essentially the same as those which result from uniform tension at infinity.

The investigation was conducted at the Illinois Institute of Technology under the sponsorship and with the financial assistance of the National Advisory Committee for Aeronautics.

In this investigation the writer was assisted by Mr. David Landsberg, Assistant Research Engineer in Experimental Stress Analysis and Mechanician in the Photoelastic Laboratory. Mr. Eugene Sevin, student assistant, worked on the separation of the principal stresses and on the isopachic stress patterns. It is a pleasure to acknowledge their wholehearted cooperation.

SYMBOLS

D	maximum width of model (fig. 1(a))
d	minimum width through discontinuity
r	radius of groove or fillet
t	thickness of model
L	axial distance between loading pins
A	minimum or net area of sections through grooves or fillets (td)
P	resultant axial load on model
p, q	principal stresses; p is algebraically maximum stress and q is algebraically minimum stress
σ_{av}	average stress across minimum area through discontinuity
σ_{max}	maximum stress at discontinuity
n	fringe order at any point

n_{unf}	fringe order in regions of uniform stress
n_{max}	maximum fringe order at discontinuity
N	order of an isopachic curve
F	fringe value of model, psi tension
k	factor of stress concentration

TEST PROCEDURE

Models

All models used in this investigation were made of Bakelite, BT-61-893, which comes in plates 12 inches by 6 inches by 1/4 inch, approximately. The blanks for the models were chosen from the center portions of the best available plates, that is, from plates which showed the smallest initial stresses. The blanks, which were a little over 4 inches in width, were thoroughly annealed at 250° to 260° F and allowed to cool slowly overnight.

The first models were 1/4 inch thick. Subsequent models were much thinner: 0.15 or 0.1 inch. The thinner models were obtained from the 1/4-inch plates by careful hand-grinding, repolishing, and reannealing.

The basic notation for the models used in this investigation is shown in figure 1(a). The nominal dimensions of the main models are shown in table I. (See also figs. 1(b) to 1(g).) The models were carefully machined on a milling attachment of a 10-inch lathe for which several special jigs were constructed.

The general procedure used in machining the grooves and fillets was to start with the smallest grooves (1/16 in. in diameter) and to introduce successively larger cutters, maintaining at the same time a constant ratio D/d . When introducing the larger cutters, in order to save machining time, the machining cuts were frequently only extended a short distance from the base of the groove. This modification of the shape of the grooves did not affect the values of k . When the largest desired value of r/d was obtained, the model was modified to give fillets for the same value of D/d . This procedure made it possible to use the same basic model for grooves and fillets. Different models, however, were required when the ratio D/d was changed for grooves.

Equipment

The main elements of the equipment used in this investigation were:

- (a) An 8-inch polariscope with a monochromatic light source (5461-A)
- (b) A straining frame with a hydraulic loading system
- (c) An annealing furnace
- (d) A camera with suitable lenses
- (e) A Babinet compensator

In addition several special jigs and fixtures were designed and built. These included jigs for milling the models and clevises for the application of the loads.

One feature of this equipment perhaps deserves special mention. This feature is found in the loading mechanism, which consists of a double, concentric tapering tank of rectangular section with suitable provisions for loading and draining. Water from the city lines is used as a dead weight. The water enters into the inner tank from which it overflows into the outer tank. The use of a small inner tank is to provide accuracy at very low loads. The two tanks form one unit suspended from the end of the loading beam which pivots about a 1/4-inch smooth lubricated pin. The whole assembly of tank and beam is carefully counter-balanced. The amount of water in each tank is read from scales, which form a background for glass tubes connected to the tank. The tanks are carefully calibrated and the accuracy of the loads is checked by means of a sensitive photoelastic dynamometer which consists of a small Bakelite tension specimen with shallow grooves.

This method of loading permits smooth continuous loading and unloading to a fraction of a pound.

Figure 2 shows a photograph of the polariscope, straining frame, and loading mechanism.

Method of Loading

All models were loaded in tension. The first tests were made with models in which the loads were applied through single pins located on the axis of the model. With this method of loading, the models showed pronounced deviations from the desired uniform tension. Accordingly, the single pin at each end was first replaced by two pins and later by four pins. Experiments were also made with friction grips and whippetree

arrangements, as shown in figure 3. Tests showed, however, that the values of k were rather insensitive to the manner of loading. The results in this report are mostly from heads with a friction grip produced by means of four equally spaced bolts having clearance in the model.

Several precautions were taken to assure that the loads applied to the model were pure axial tensions. In order to eliminate bending and twisting one end of the model was supported on a smooth hard ball. Also in order to eliminate small eccentricities, the load was applied through a clevis which could be adjusted relative to the axis of the model.

Time Stresses

A major cause of error in the determination of boundary stresses from Bakelite models arises from the compressive stresses, known as time stresses, which form rather rapidly on the edges of the model independently of the applied loads. In order to reduce or to eliminate these effects the work at the polariscope had to be done without interruption or delay. Models were always photographed within 1 hour, or at most $1\frac{1}{2}$ hours, after machining. In general, good success was obtained in reducing and often eliminating entirely the time stresses.

Occasionally, unusual difficulties were encountered in the alinement of the model which delayed the photography with consequent distortions in the boundary stresses. In such cases the model was given a high-temperature annealing (260° F) overnight, and the model was rephotographed the next morning, often with good results.

The general procedure was to develop the negatives immediately after photographing the stress pattern and before the model was much affected by time stresses.

FACTORS OF STRESS CONCENTRATION

Definition

The factor of stress concentration k is defined by the expression,

$$k = \frac{\sigma_{\max} \text{ in the section through discontinuity}}{\sigma_{av} \text{ or nominal stress } P/A} \quad (1)$$

From equation (1)

$$\sigma_{\max} = k\sigma_{av} \quad (2)$$

Thus, the factor of stress concentration as defined here represents a correction factor to the usual manner of calculating stresses.

Fringe-Value Method

In terms of n and F ,

$$k = \frac{n_{\max} F}{P/A} \quad (3)$$

Equation (3) is one basic expression for the calculation of factors of stress concentration. This equation contains the fringe value F . The method based on equation (3) will be referred to as the "fringe-value method."

Accuracy of Fringe-Value Method

From equation (3) it follows that the accuracy of the values of k depends on the accuracy of the four quantities: A , P , F , and n_{\max} .

Accuracy of the area A . Since the area A of the net section was fairly large, ranging from 0.45 to 0.2 square inch, approximately, the accurate determination of values of A presented no difficulty.

Accuracy of the loads P . The precautions taken in the accurate determination of the loads P have already been discussed. These loads ranged from a minimum of 150 to 550 pounds, approximately. The probable error in these loads was not greater than 1 percent.

Accuracy of the fringe value F . The constant F was determined for each model from two different calibration members cut from the model under investigation: A tension member and a circular disk under diametral loads.

The procedure for the determination of F from a tension model is already well-known and is fully described in the literature. The use of the circular disk is relatively new. This method has certain advantages over the tension model. It provides an extremely sensitive type of stress pattern from which the fringe order n_c at the center of the disk corresponding to a definite diametral load P can be determined with great accuracy. For such a disk the fringe value F is given by

$$F = \frac{2P}{\pi R t n_c} \quad (4)$$

(equation (4.71) of reference 1) in which R is the radius of the disk and t is its thickness. The error in F is not believed to exceed 1 percent.

Accuracy of n_{max} . - The general procedure in the determination of n_{max} at the grooves or fillets was to make an enlargement of the stress pattern and to extrapolate the $p - q$ curve to the free boundary of the groove or fillet.

The extrapolation was frequently performed several times to different scales in such a way that the extrapolated branch of the $p - q$ curve was held fairly close to the tangent at the last definite point on the curve.

With all these precautions the possibility of an error of 1 fringe in 10, or proportionate amounts at other fringe orders, must be assumed to exist for the small cutters, $2r = 1/16$ inch and $2r = 3/32$ inch. These errors come primarily from the possible error in locating the position of the free boundary.

Further steps to increase the accuracy of k . - In order to reduce the errors in k as much as possible, two major steps were taken:
(a) For one and the same model, two different loads were frequently used;
(b) for critical values of k , two and sometime three different models under different loads were used.

All values of k were determined from photographed stress patterns. The general procedure was to use bright backgrounds. Occasionally, however, both dark and bright backgrounds were used.

Photographic Method

It is possible to determine the value of k without measuring fringe values or even loads. This method may be called the "photographic method" to distinguish it from the fringe-value method. The photographic method rests on the assumption that the stresses some distance from the discontinuity are uniform and that they can be accurately determined optically. The basic equation in this method is

$$k = \frac{n_{max}}{n_{unf} D / d} \quad (5)$$

However, because of the fact that the values of n_{unf} were, in this investigation, inherently low - of the order of magnitude of one fringe - the accuracy of this method was not believed to be as good as that of the fringe method. Another complication arose from the fact

that generally no true uniform tension was developed in the models. The use of an auxiliary narrow shank to obtain a uniform stress of a relatively high value was in this investigation impractical. The fringe-value method was therefore adopted and used throughout the investigation although several values of k were calculated by both methods with substantial agreement. (See table II.)

PRINCIPAL STRESSES

Except for points on free boundaries, the photoelastic stress patterns provide only the values of $p - q$, that is, the values of the difference between the principal stresses, but not the principal stresses themselves. A variety of methods exist for the determination of the principal stresses from photoelastic data. Some of these, like Filon's graphical integration and the shear difference method, require the use of isoclinics (reference 2, chs. 8 and 9). Others require measurements of the changes in the thickness of the model produced by the stresses (reference 1, ch. 7). These deformations are obtained by means of sensitive instruments which are known as lateral extensometers.

A third group of methods utilizes only the free boundary stresses obtainable from the stress patterns and requires neither isoclinics nor measurements with lateral extensometers. To this group belong the slope-equilibrium method (reference 2, ch. 7) for the determination of p and q on sections of symmetry and the numerical solution of Laplace's equation for the evaluation of $p + q$ at any interior point (reference 1, ch. 8).

After considerable preliminary work with several of the methods mentioned above, two methods were chosen and used to obtain the results given in this report:

- (a) The slope-equilibrium method.
- (b) The numerical solution of Laplace's equation with conformal transformations (reference 1, ch. 9).

The theory of these methods as well as numerous examples showing their application can be found in the writer's books on photoelasticity (references 1 and 2).

ISOPACHIC PATTERNS

An isopachic curve is a curve of constant $p + q$. Such curves are analogous to the fringes in the photoelastic stress patterns which are the loci of constant values of $p - q$. The isopachic patterns were constructed from the values obtained from the numerical solution of Laplace's

equation by iteration. In general, the isopachic patterns provide the necessary and sufficient data from which $p + q$ at every point in the bar can be calculated. Specifically,

$$p + q = CN \quad (6)$$

in which N is the order of the isopachic curve and C is a constant for the model. The curves were constructed in a manner to make the constant C equal to the fringe value F of the model.

By combining the values of $p + q$ from the isopachic patterns with the values of $p - q$ from the stress pattern the principal stresses p and q can be found at any point.

RESULTS AND DISCUSSION

Results

Factors of stress concentration.- Values of k for grooves with $D/d = 1.5$ and $D/d = 2$ are given in table III and in the curves of figure 4. Similar results for fillets are given in table IV and in the curves of figure 5. Figures 6 and 7 show comparative curves for grooves and fillets for $D/d = 1.5$ and $D/d = 2$, respectively.

Principal stresses.- The principal stresses p and q for the sections through the grooves are given in figures 8 and 9.

Isopachic patterns.- Figure 10 shows isopachic patterns for several basic cases of grooved bars.

Typical photoelastic stress patterns for fillets and grooves are shown in figures 11 to 15. Figure 15 shows the clarity of boundary stresses obtained for a 1/16-inch cutter. In this pattern the distance between the last two fringes is less than 0.002 inch. In many cases it was about 0.001 inch.

Because of this extremely sharp gradient of the stresses at the boundaries of the discontinuities, lateral extensometers were ruled out as suitable instruments for the determination of the sums of the principal stresses.

General Observations

In both grooves and fillets factors of stress concentration increase sharply as r/d becomes less than 0.05.- For grooves (fig. 4) the increase in k corresponding to a change in r/d from 0.05 to 0.02

is 46 and 52 percent, approximately, for $D/d = 1.5$ and $D/d = 2$, respectively.

The corresponding values for fillets (fig. 5) are 34 and 37 percent, approximately. The trend for fillets is the same as for grooves. However, the quantitative effect on k resulting from a reduction in r/d is smaller for fillets than for grooves.

In both fillets and grooves, values of k increase with D/d . Inspection of figures 4 and 5 shows that for both grooves and fillets, at $r/d = 0.02$, the effect of changing D/d from 1.5 to 2 is to produce an increase of 20 percent, approximately, in the value of k .

Effect of grooves on stress concentration is considerably greater than effect of fillets; that is, for the same D/d and r/d grooves yield larger factors of stress concentration. The effect of grooves increases as r/d decreases. This is clearly shown by figures 6 and 7. Specifically, at $r/d = 0.02$ and $D/d = 1.5$ grooves yield values of k which are 52 percent greater than those produced by fillets. For the same value of r/d and $D/d = 2$, the increase is 46 percent.

For $r/d = 0.05$ the corresponding increase is 35 percent for $D/d = 1.5$ and 33 percent for $D/d = 2$. The effect is thus essentially the same for both values of D/d .

Factors of stress concentration for grooves and fillets are essentially the same for several types of loading employed. Table V shows no significant change in the values of k for the several methods of loading, even for $r/d = 0.0109$ and 0.0165 , which are extremely sensitive cases. For $r/d = 0.0109$ the factor varies from 7 to 7.1, approximately, for loads applied through four pins - two outside pins and two inside pins - and by means of a friction grip. This is a negligible effect well within the experimental error. It should also be observed that the same constancy of k is found in the short 9-inch plate and in the longer 12-inch plate. Since the technique and the precautions taken were the same throughout the investigation, it must be concluded that the stress concentration factors are not materially affected by the manner of loading, and that, for the particular types of loading employed, the values of k are essentially equal to those produced by pure tension at infinity.

Previous work has shown that the values of k are a function of L/D (fig. 1(a)) at least where the loads are applied by means of a single pin. Caution must therefore be exercised not to give the above result too great a generality. It is reasonably certain that for bars with small ratios of L/D , the factors of stress concentration would show considerable deviation. This aspect needs further study and clarification.

Figure 13 shows that the modification of the shape of the grooves has no effect on the values of k .

Large stresses penetrate only a very small distance into material.-

Thus, for $D/d = 1.5$ and $r/d = 0.011$ approximately, the value of p for grooves drops from a maximum of $7.07P/A$ to about $3.5P/A$ in a distance of $r/2$ measured from the root of the groove (see fig. 8(a)).

Transverse stresses.- Transverse stresses q (figs. 8 to 10) are all tensile and they reach their maximum values at points very close to the root of the grooves. The distance from the root of groove to the maximum value of q is of the order of magnitude of $r/2$. In general, the maximum values of q increase as r/d decreases. At $r/d = 0.011$ and $D/d = 1.5$, $q_{\max} = 1.5P/A$, approximately.

Precision

The precision of photoelastic results differs considerably for different aspects of the problem, such as values of $p - q$ at interior points, boundary values, and so on. The precision may further differ for one and the same aspect. Thus, the accuracy of $p - q$ depends in a large measure on the magnitude of the fringe order n at the point under consideration.

Errors in $p - q$.- The highest accuracy is, in general, obtainable for $p - q$ at interior points. Here the errors can be reduced to a fraction of 1 percent.

Errors in values of k .- The next highest accuracy obtainable photoelastically is for boundary values. In grooves and fillets with a value of r/d greater than 0.05 there is no difficulty in obtaining stress patterns with a fringe order of at least 10 at the discontinuity determined accurately to within one-fourth or even one-eighth of a fringe.

Since the major errors in k are due to errors in the value of the maximum fringe order, this is tantamount to saying that for $r/d \geq 0.05$ the error in k can be kept to about 2 percent.

However, when studying factors of stress concentration for values of r/d less than 0.05, by means of relatively small models in which cutters 1/8 or 1/16 inch in diameter are employed, the errors in the maximum fringe order may be considerably greater. As already pointed out, the large stresses at sharp grooves are confined to a very small space. Specifically, for a cutter 1/16 or 3/32 inch in diameter, there may be three or four fringes in a space of 0.006 to 0.008 inch. The fringes are thus very crowded and have an extremely sharp gradient. The determination of an accurate value of the maximum fringe order depends

on the ability to locate with precision the boundary of the groove or fillet. An error in the position of the true boundary of 0.002 inch or even 0.001 inch is sufficient to introduce an error of as much as one-half to one fringe, depending on the magnitude of the maximum fringe order. The resulting errors in k may under these conditions reach values from 5 to 10 percent. This would seem to be the probable range of error in the values of k for $r/d \leq 0.02$.

An examination of all the factors entering into the calculation of k would lead one to believe that the values of k obtained photoelastically and given in this report are conservative values.

Errors in principal stresses.- As far as the principal stresses are concerned, here again one must distinguish between the accuracy in the p stresses and the q stresses, that is, between the accuracy of the large stresses and the small stresses. The accuracy of the large stresses is relatively high. Specifically, the errors in the values of p , when they are greater than P/A , are probably of the same order of magnitude as the errors in the values of k .

The general shape of the p curves given in this report is believed not to differ much from their true shapes. These curves have been constructed to meet essentially all the requirements of statics and continuity. The static check in the distribution of p is within 2 to 6 percent.

The position of the maximum q stresses may be assumed to be very accurately located. They were found from the zero isoclinics. The magnitudes of the q stresses are relatively small and their accuracy is therefore inherently lower than that of the p stresses. However, these stresses have been determined in several ways with substantial agreement.

Comparison of Theoretical and Photoelastic Values of k for Deep Grooves in Tension

Figure 16 shows a comparison of the photoelastic values of k with those obtained by Neuber (reference 3). It should be observed that Neuber's curve is based on theoretical values of k for deep and shallow grooves and that in between these extremes this curve represents results from an interpolation.

Inspection of the curves shows that for $D/d = 1.5$ the two curves practically coincide. For $D/d = 2$ the experimental results are

somewhat higher than those given by Neuber. It is believed that the photoelastic values represent the better approximation.

Illinois Institute of Technology
Chicago 16, Ill., April 7, 1949

REFERENCES

1. Frocht, Max Mark: Photoelasticity. Vol. II. John Wiley & Sons, Inc., 1948.
2. Frocht, Max Mark: Photoelasticity. Vol. I. John Wiley & Sons, Inc., 1941.
3. Neuber, H.: Kerbspannungslehre: Grundlagen für genaue Spannungsrechnung. Julius Springer (Berlin), 1937. (Also available as Translation 74, The David W. Taylor Model Basin, U. S. Navy, Nov. 1945.)

TABLE I.- NOMINAL DIMENSIONS OF MAIN MODELS

[For notation see fig. 1(a)]

Model	D (in.)	d (in.)	L (in.)	t (in.)	D/d	L/D	(psi ^F tension)
A, grooves	2.45	1.63	$8\frac{1}{4}$	0.147	1.5	3.4	605
B, fillets	2.40	1.60	$8\frac{1}{4}$	0.147	1.5	3.4	605
B', fillets	2.30	1.53	$6\frac{1}{2}$	0.102	1.5	2.8	868
C, grooves	4.25	2.83	$10\frac{1}{8}$	0.158	1.5	2.4	546
D, fillets	4.00	2.70	$10\frac{1}{8}$	0.108	1.5	2.5	798
E, fillets	4.00	2.00	$10\frac{1}{8}$	0.108	2.0	2.5	798
F, grooves	3.90	1.95	$10\frac{3}{4}$	0.150	2.0	2.8	585
G, fillets	3.80	1.90	$10\frac{3}{4}$	0.150	2.0	2.8	585
H, grooves	1.75	1.17	$10\frac{1}{8}$	0.085	1.5	5.8	1015



TABLE II.- COMPARATIVE VALUES OF FACTOR OF STRESS
 CONCENTRATION k FROM PHOTOGRAPHIC
 AND FRINGE-VALUE METHODS

D/d	r/d	$\frac{2r}{\text{(in.)}}$	n_{unf}	n_{max}	k	
					Fringe-value method	Photo-graphic method
1.500	0.0109	1/16	0.90	9.05	7.09	6.65
1.500	0.0165	3/32	0.93	7.45	5.67	5.35
1.508	0.0222	1/8	1.09	7.45	4.82	4.72



TABLE III.- DATA FOR STRESS CONCENTRATION FACTOR k FOR
THREE MODELS WITH GROOVES

D/d	r/d	2r (in.)	A = td (sq in.)	P (lb)	$\sigma_{ay} = P/A$ (psi)	n _{max}	k
Model A							
1.492	0.0187	1/16	0.243	159	654	5.84	5.40
1.494	0.0281	3/32	0.242	187	771	5.76	4.52
				249	1029	7.64	4.50
1.500	0.038	1/8	0.241	285	1181	7.8	4.00
1.505	0.0475	5/32	0.241	303	1259	7.5	3.63
				433	1800	10.82	3.64
1.510	0.057	3/16	0.238	321	1348	7.45	3.34
1.507	0.067	7/32	0.239	250	1046	5.55	3.21
				512	2147	11.5	3.23
1.502	0.0768	1/4	0.237	264	1113	5.55	2.97
				492	2074	10.1	2.99
Model C							
1.50	0.0109	1/16	0.452	347	768	9.95	7.09
1.51	0.011	1/16	0.449	314	700	9.05	7.07
1.50	0.0165	3/32	0.446	319	716	7.45	5.67
				332	745	7.70	5.65
1.508	0.0222	1/8	0.444	374	842	7.45	4.82
1.508	0.0334	3/16	0.443	370	835	6.35	4.15
				423	954	7.33	4.19
1.508	0.0447	1/4	0.442	465	1050	7.35	3.80
				524	1184	8.32	3.84
Model F							
2.001	0.0159	1/16	0.295	250	845	10.4	7.20
2.002	0.0238	3/32	0.295	273	925	8.7	5.51
2.003	0.0318	1/8	0.295	344	1167	9.55	4.78
2.003	0.0397	5/32	0.295	438	1486	11.18	4.40
2.004	0.0477	3/16	0.295	442	1498	10.4	4.06
2.000	0.0638	1/4	0.294	433	1473	9.13	3.62
2.001	0.0806	5/16	0.289	413	1430	8.2	3.35
2.001	0.0967	3/8	0.289	533	1845	9.7	3.08

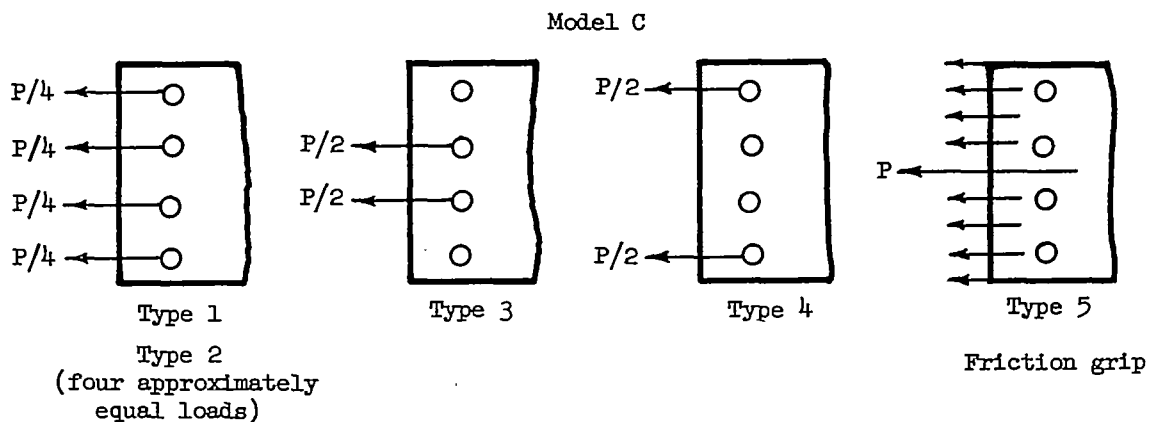


TABLE IV.- DATA FOR STRESS CONCENTRATION FACTOR k FOR
THREE MODELS WITH FILLETS

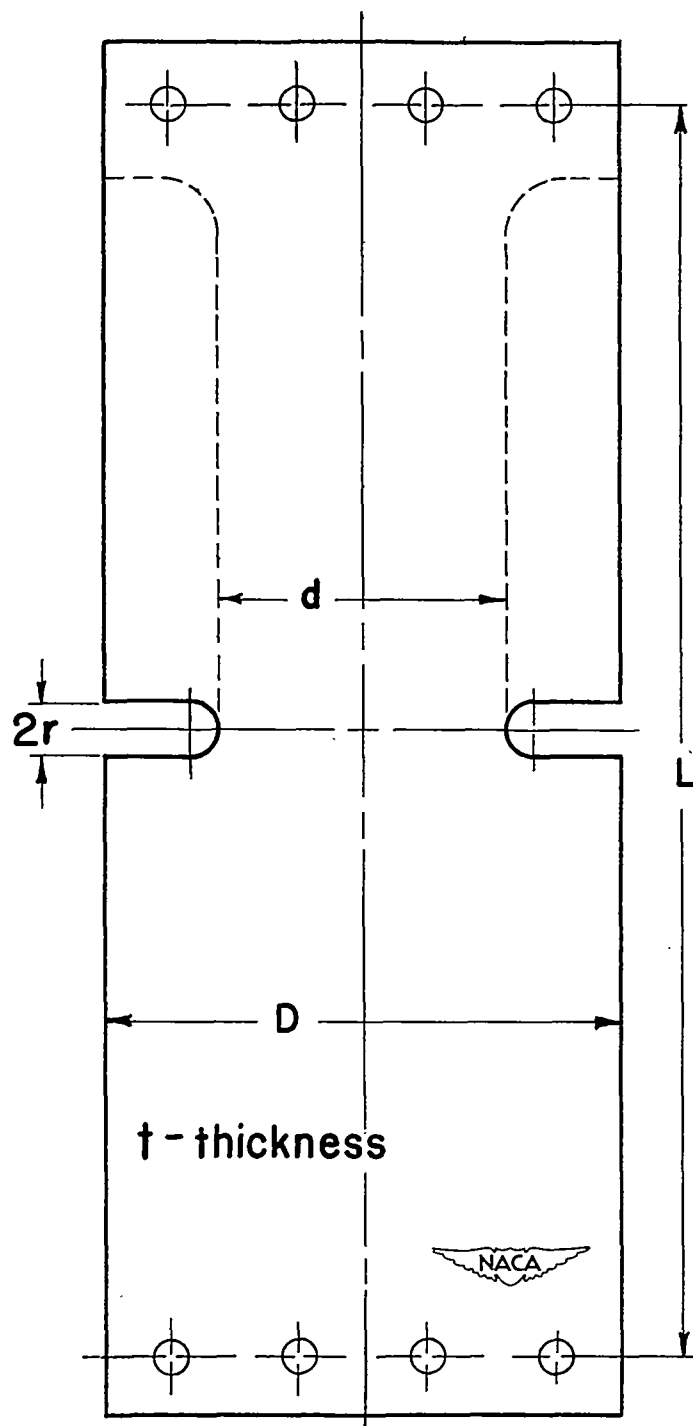
D/d	r/d	$2r$ (in.)	$A = td$ (sq in.)	P (lb)	$\sigma_{ay} = P/A$ (psi)	n_{max}	k
Model B							
1.50	0.0488	5/32	0.234	481	2060	8.85	2.60
1.50	0.0586	3/16	0.234	475	2027	8.5	2.54
1.50	0.0683	7/32	0.234	487	2078	8.35	2.43
1.50	0.0780	1/4	0.235	268	1142	4.35	2.30
Model D							
1.500	0.0116	1/16	0.293	364	1242	6.58	4.22
1.504	0.0118		0.287	430	1497	7.85	4.20
1.499	0.0174	3/32	0.291	501	1721	7.81	3.62
1.504	0.0176		0.287	477	1660	7.48	3.60
1.499	0.0232	1/8	0.291	521	1790	7.54	3.36
				525	1804	7.55	3.34
1.499	0.0348	3/16	0.291	526	1807	6.75	2.98
Model E							
2.005	0.0157	1/16	0.2128	289	1358	8.06	4.75
2.005	0.0238	3/32	0.2128	343	1612	7.8	3.86
2.005	0.0317	1/8	0.2128	373	1750	7.55	3.45
2.003	0.0472	3/16	0.2149	339	1577	6.07	3.08
2.010	0.0628	1/4	0.2149	374	1740	6.24	2.86
				434	2020	7.3	2.88



TABLE V.- EFFECT OF DIFFERENT TYPES OF LOADING
ON VALUES OF STRESS CONCENTRATION FACTOR k

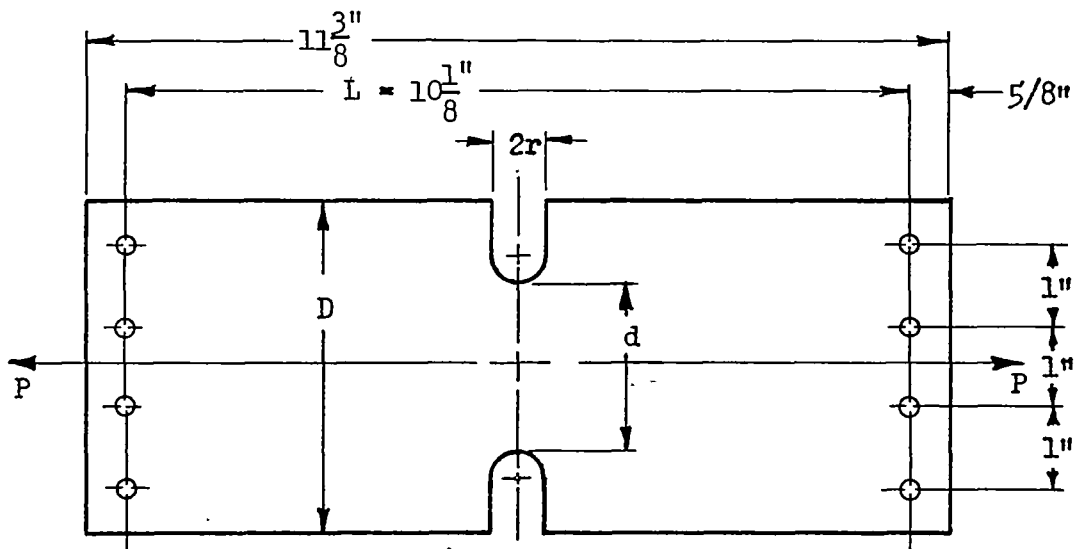


Type of head	k	D/a	r/a	$2r$ (in.)	L/D
2	7.03	1.50	0.0109	1/16	2.4
3	7.12				
4	7.12				
5	7.09				
3	5.74	1.50	0.0165	3/32	2.4
4	5.74				
5	5.67				
1	4.95	1.508	0.0222	1/8	2.4
3	5.00				
4	4.95				
5	4.82				

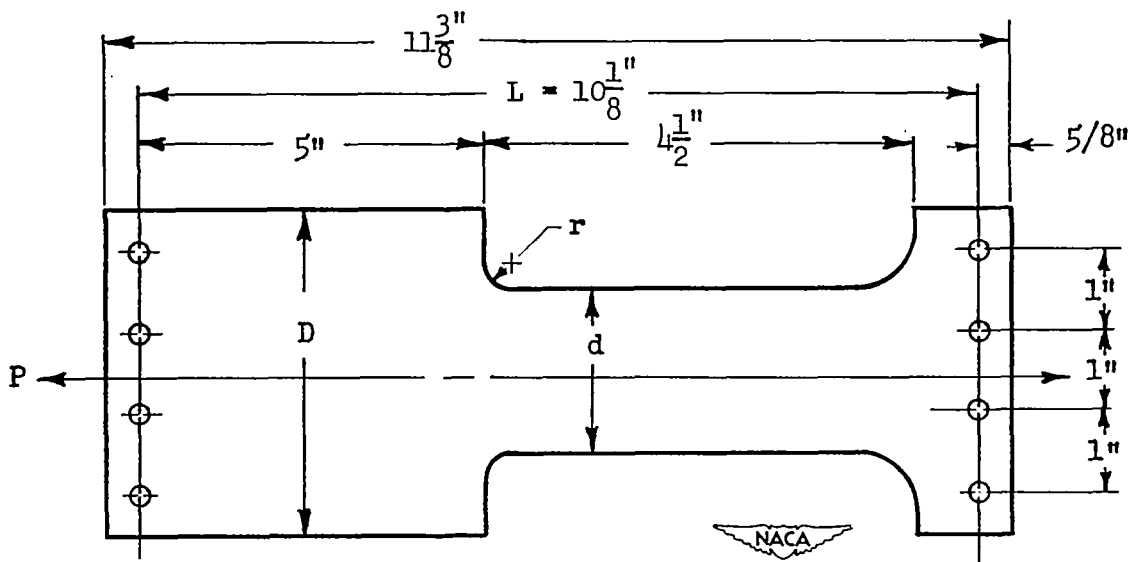


(a) Basic notation.

Figure 1.- Sketches showing basic notation for models and dimensions for models A, B, C, D, E, and F.

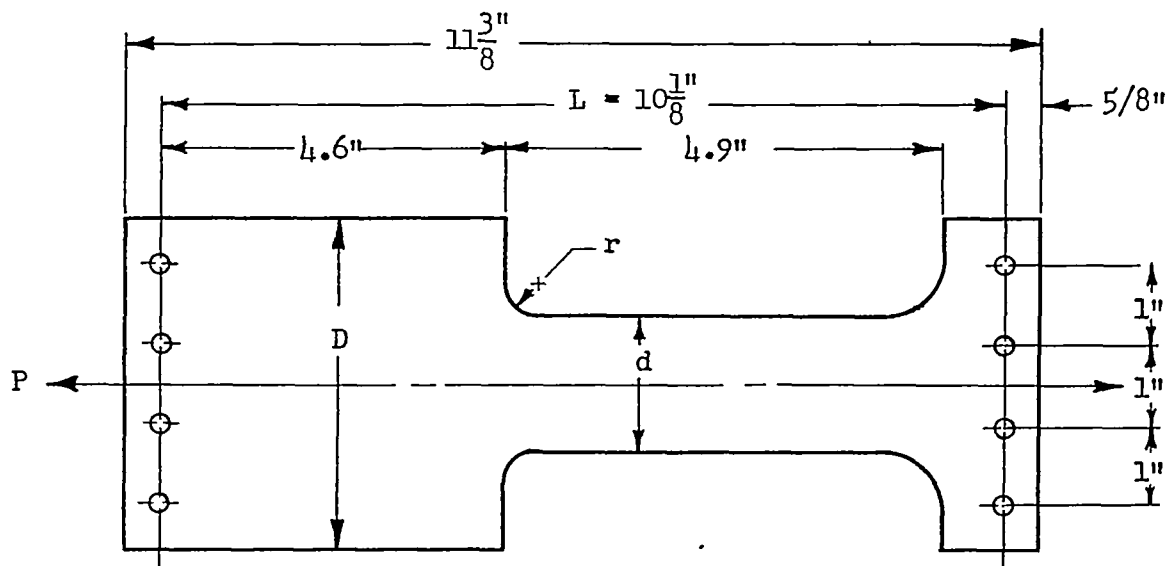


(d) Model C. $t = 0.158$ inch; $F = 546$ psi tension; $D = 4.230$ to 4.285 inches; $d = 2.800$ to 2.860 inches.

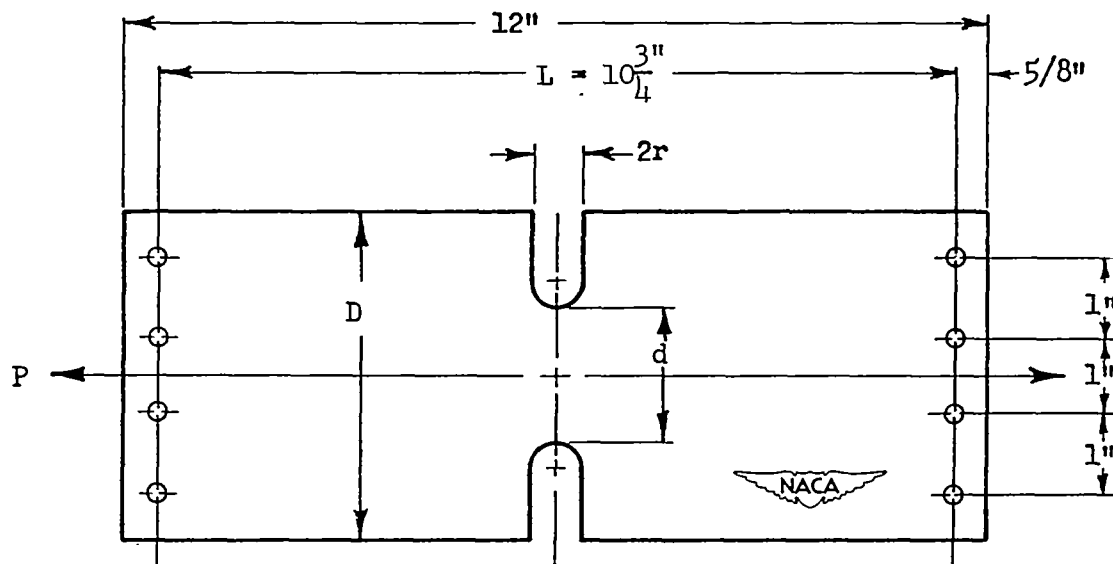


(e) Model D. $t = 0.108$ inch; $F = 798$ psi tension; $D = 4.04$ to 4.07 inches; $d = 2.695$ to 2.713 inches.

Figure 1.- Continued.



(f) Model E. $t = 0.108$ inch; $F = 798$ psi tension; $D = 3.95$ to 4.00 inches; $d = 1.97$ to 1.99 inches.



(g) Model F. $t = 0.150$ inch; $F = 585$ psi tension; $D = 3.879$ to 3.937 inches; $d = 1.939$ to 1.968 inches.

Figure 1.- Concluded.

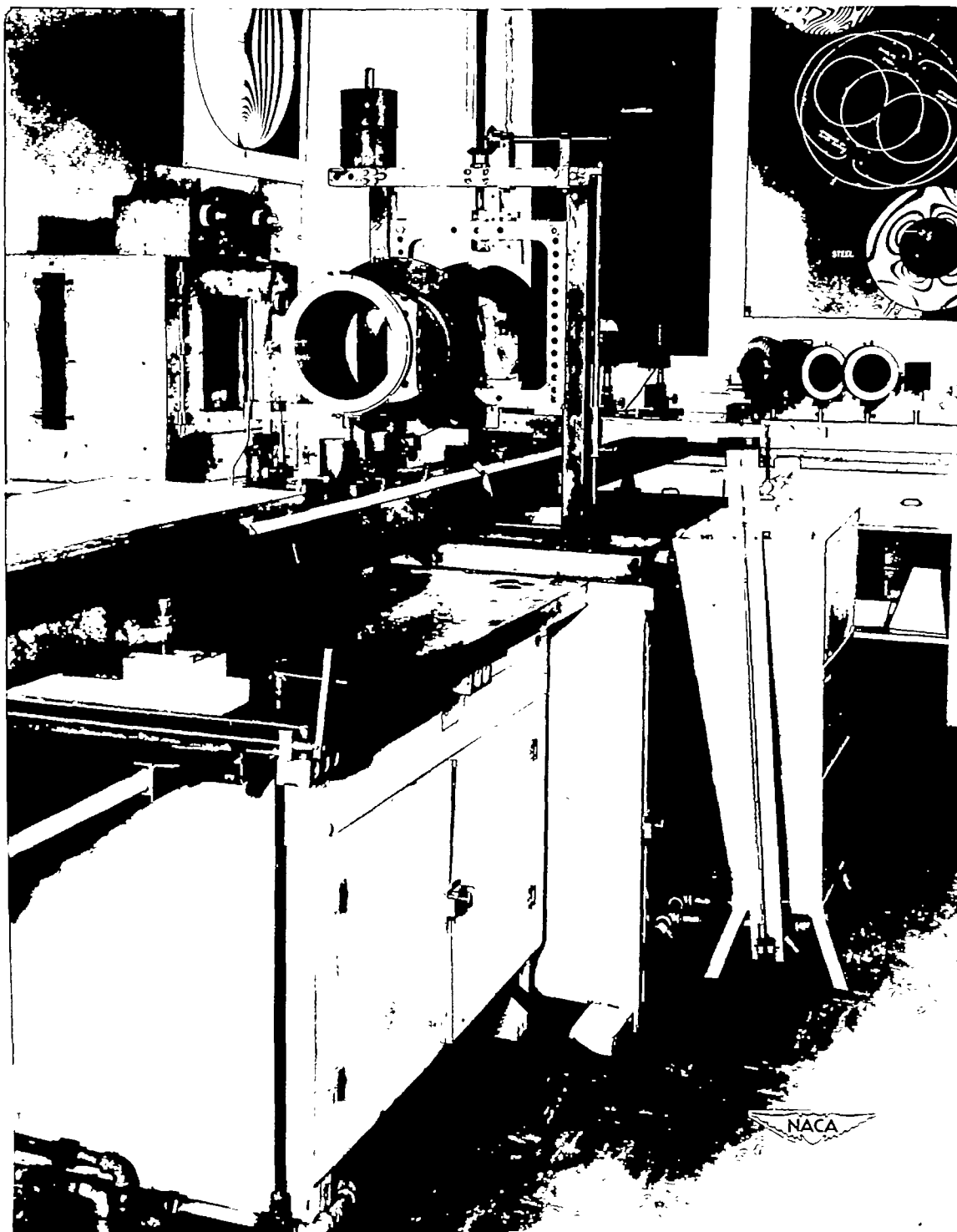
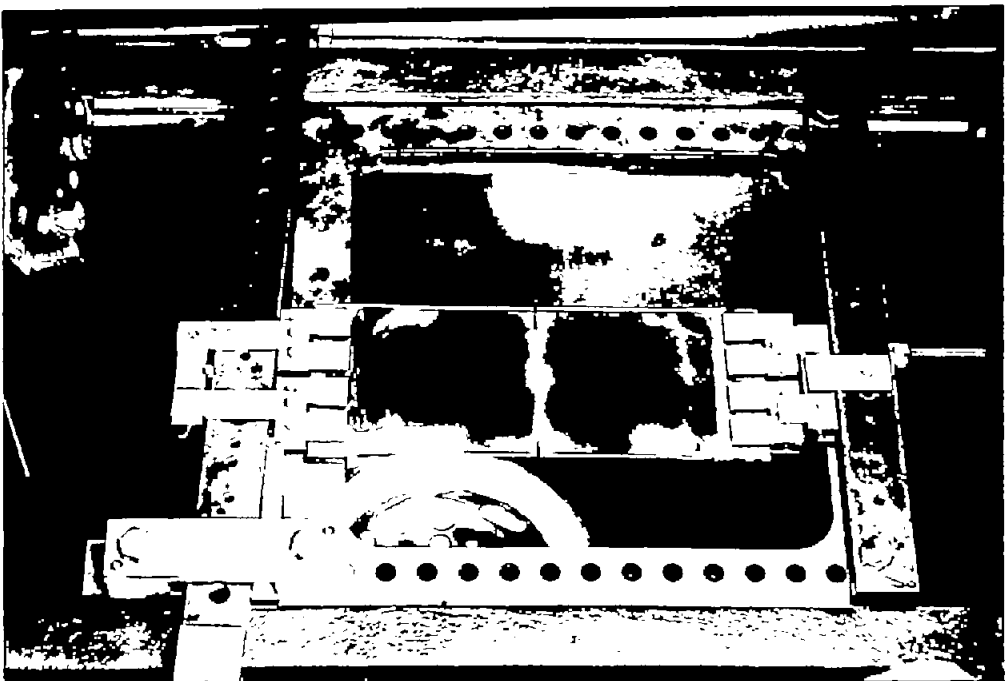
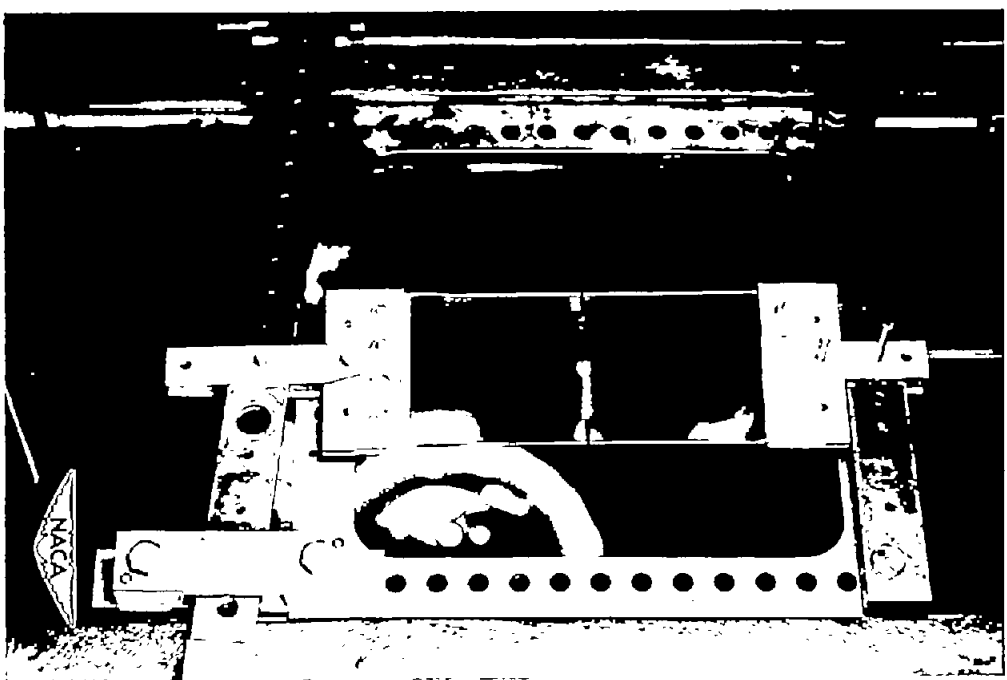


Figure 2.- Laboratory view showing polariscope, straining frame, hydraulic loading system, and furnace. A Bakelite model of a bar with sharp fillets is in the testing machine.



(a) Whippletree head.



(b) Friction-grip head.

Figure 3.- Grooved model under two types of loading.

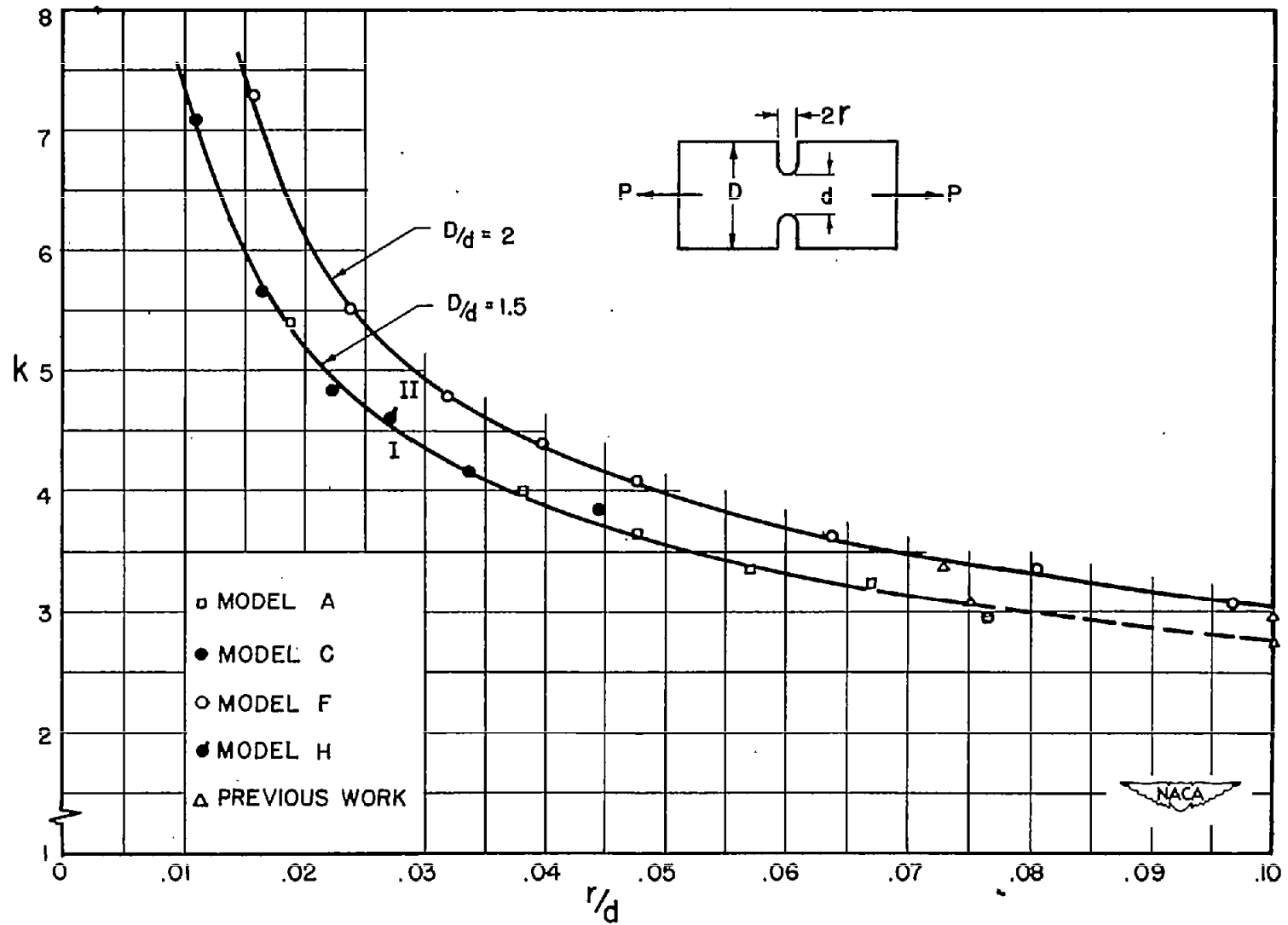


Figure 4.- Curves of stress concentration factor k for a bar with grooves in tension.

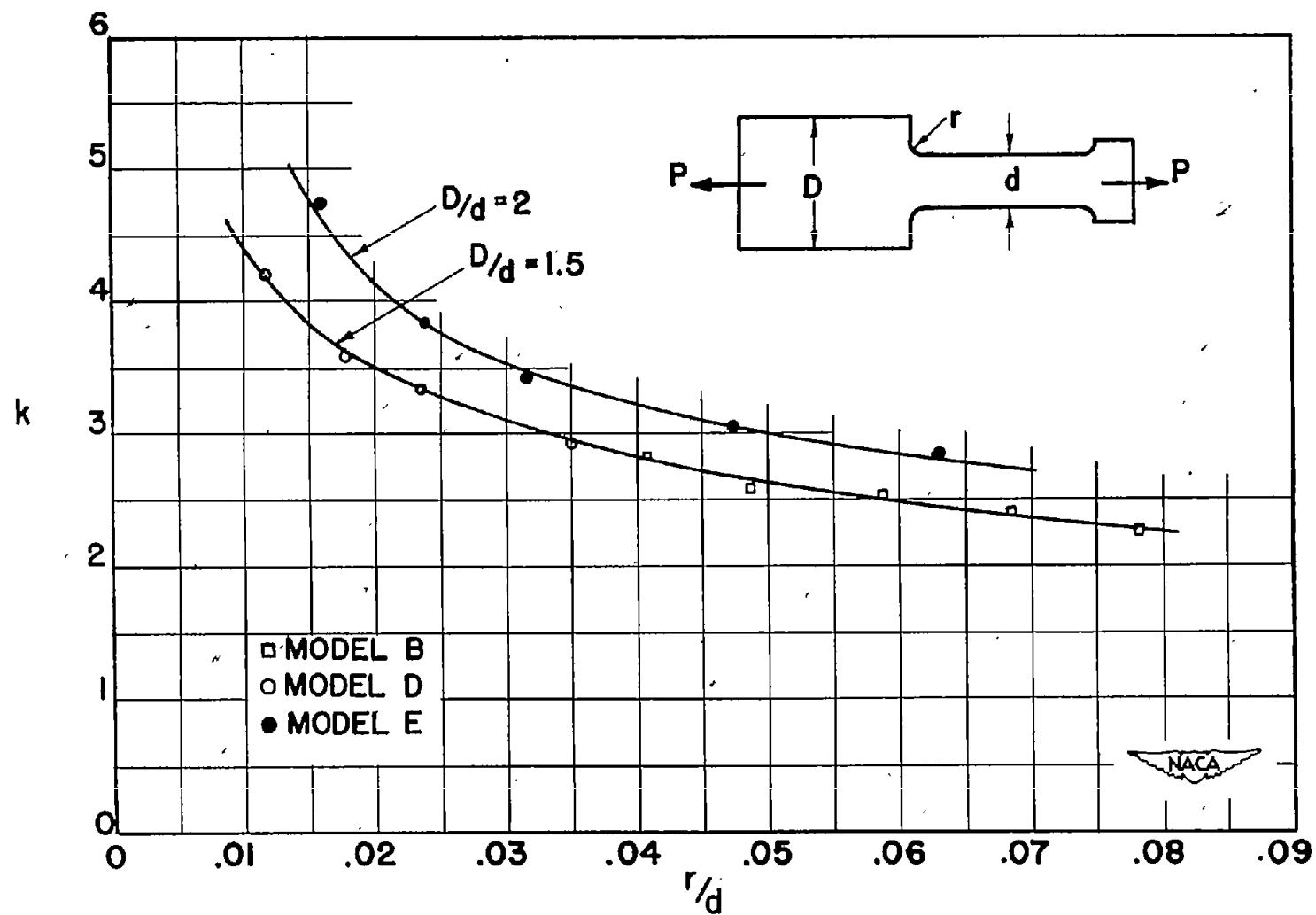


Figure 5.- Curves of stress concentration factor k for a bar with fillets in tension.

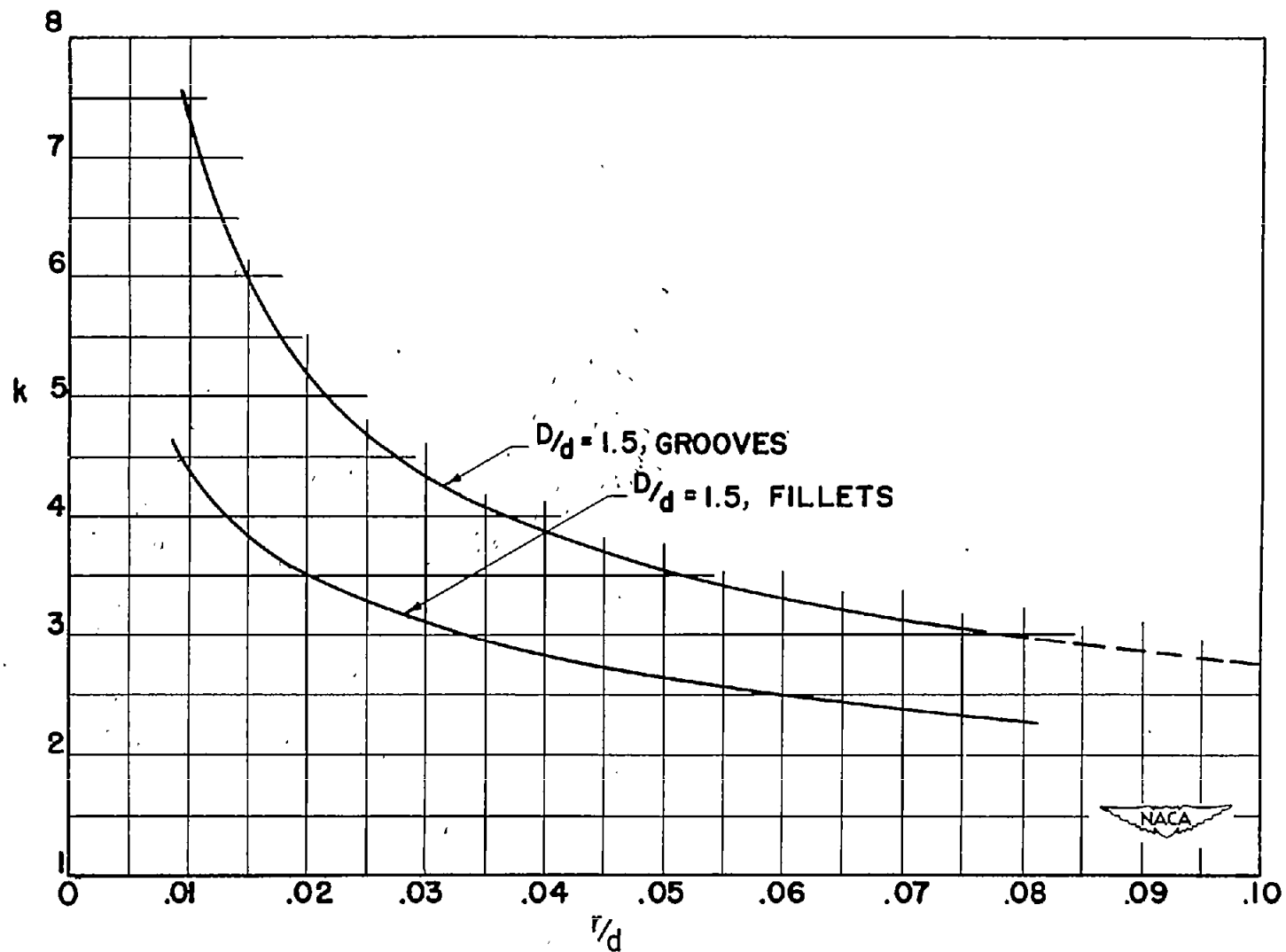


Figure 6.- Comparative curves of k for bars in tension containing grooves or fillets. $D/d = 1.5$.

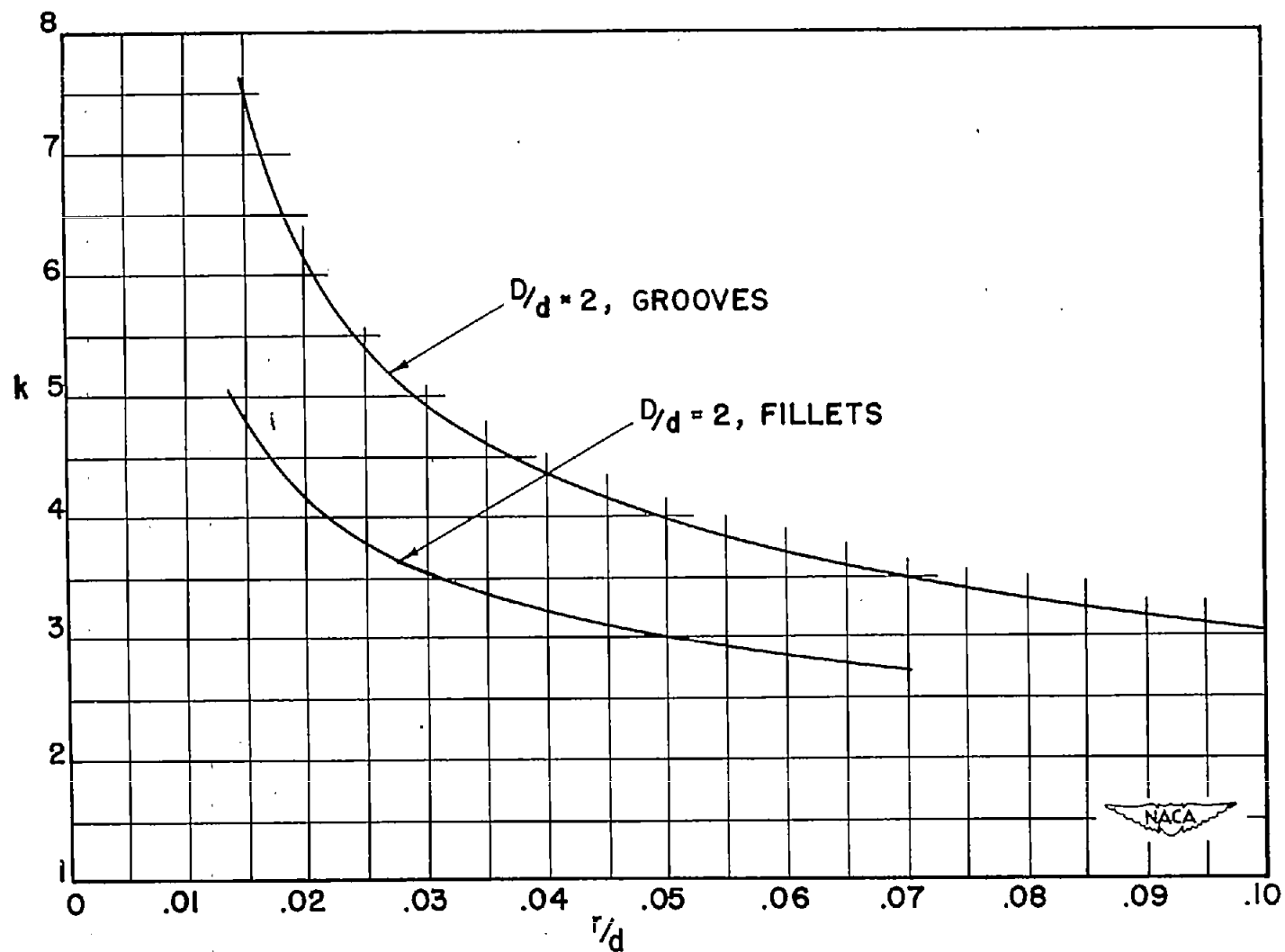
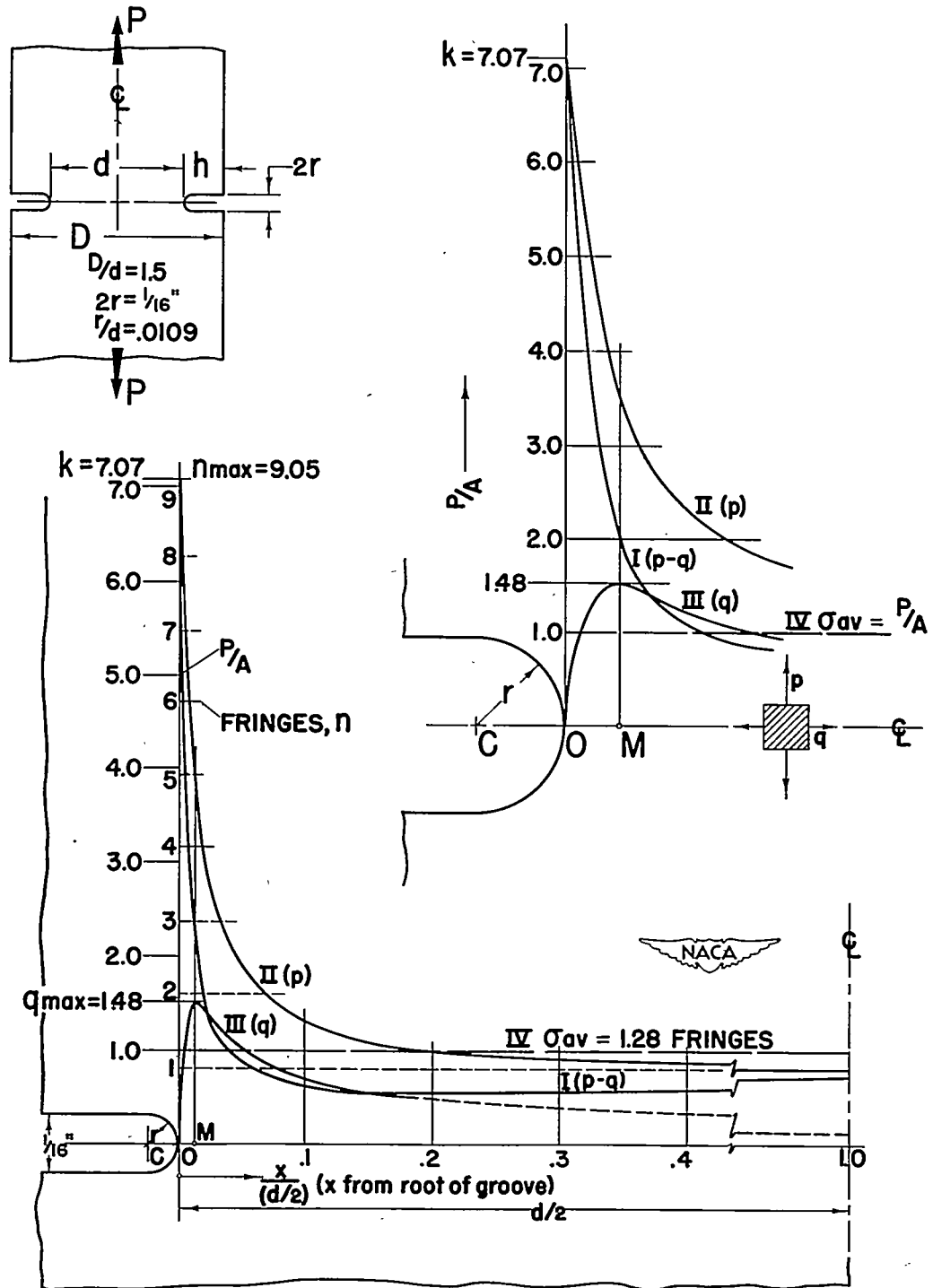
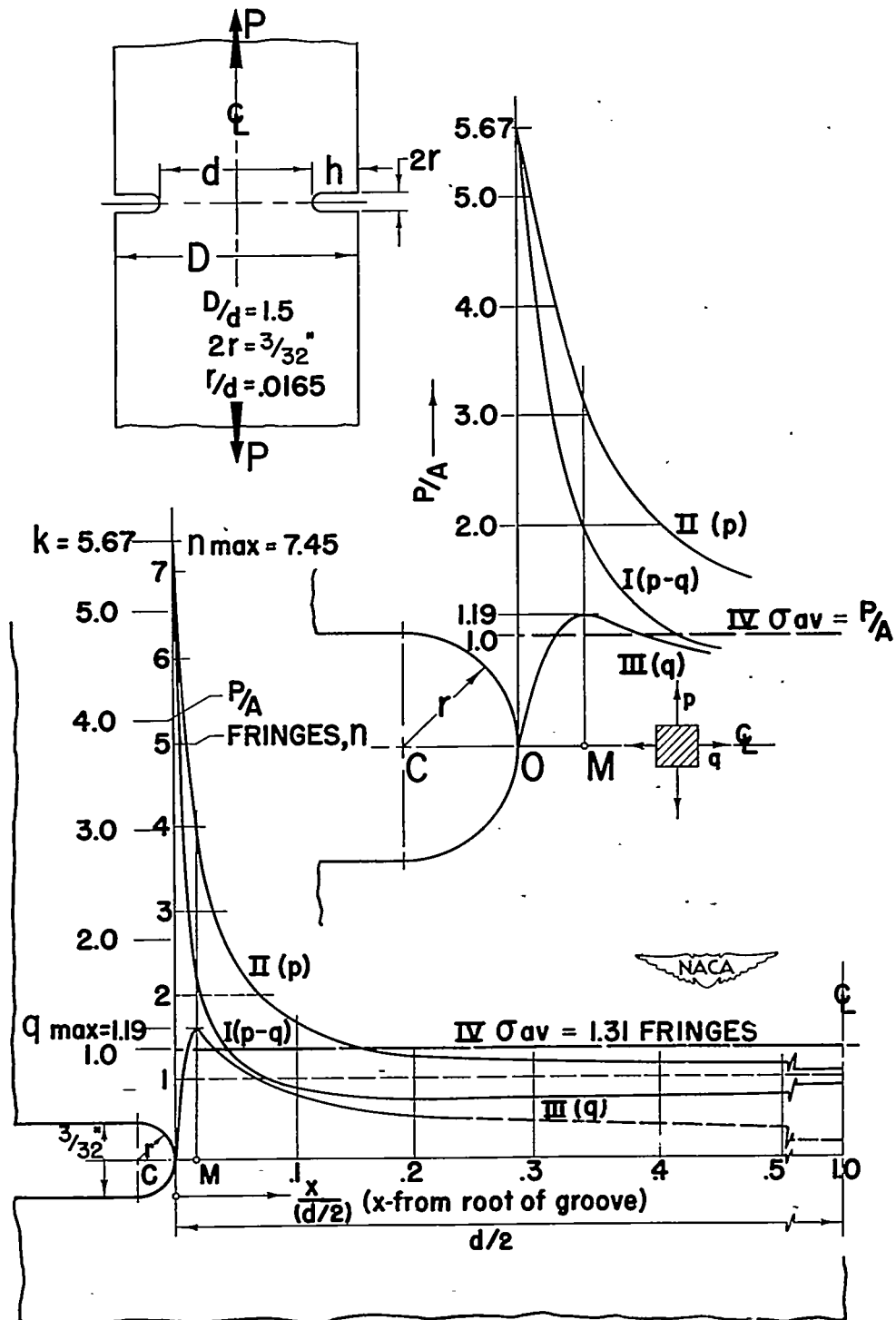


Figure 7.- Comparative curves of k for bars in tension containing grooves or fillets. $D/d = 2$.



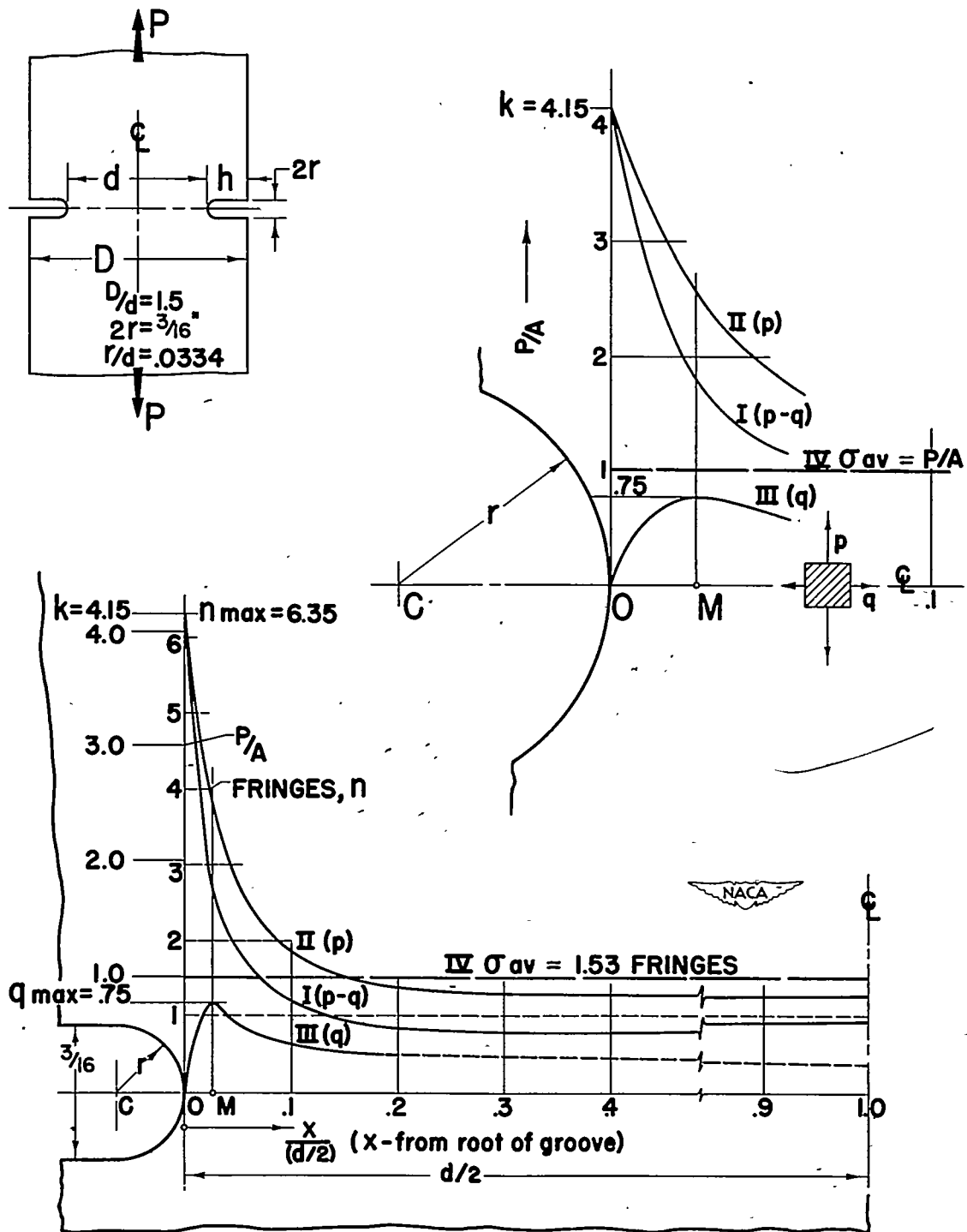
(a) Model C; $D/d = 1.5$; $r/d = 0.0109$; $2r = 1/16$ inch.

Figure 8.- Distribution of principal stresses p and q for section through grooves obtained by slope-equilibrium method.



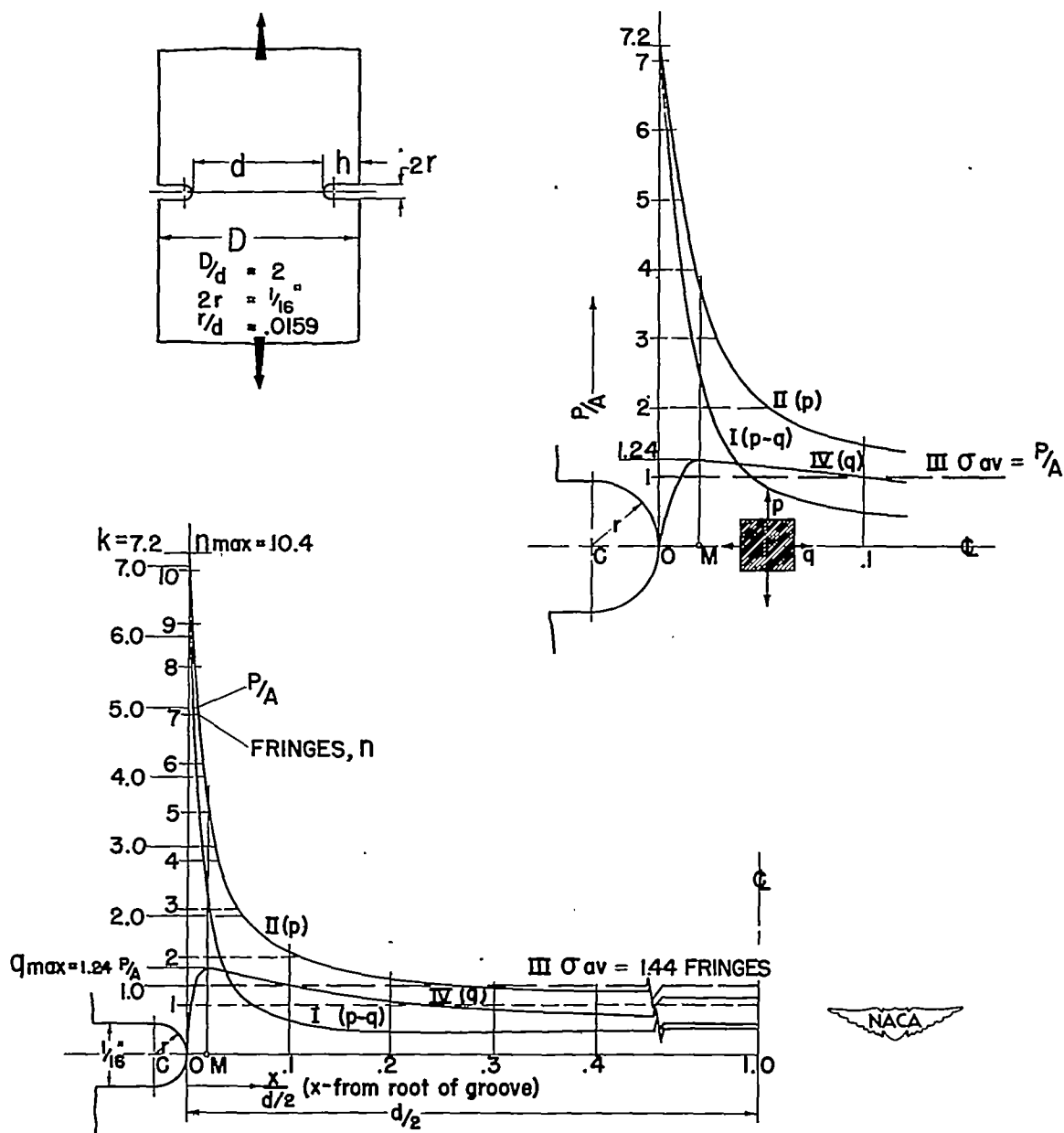
(b) Model C; $D/d = 1.5$; $r/d = 0.0165$; $2r = 3/32$ inch.

Figure 8.- Continued.



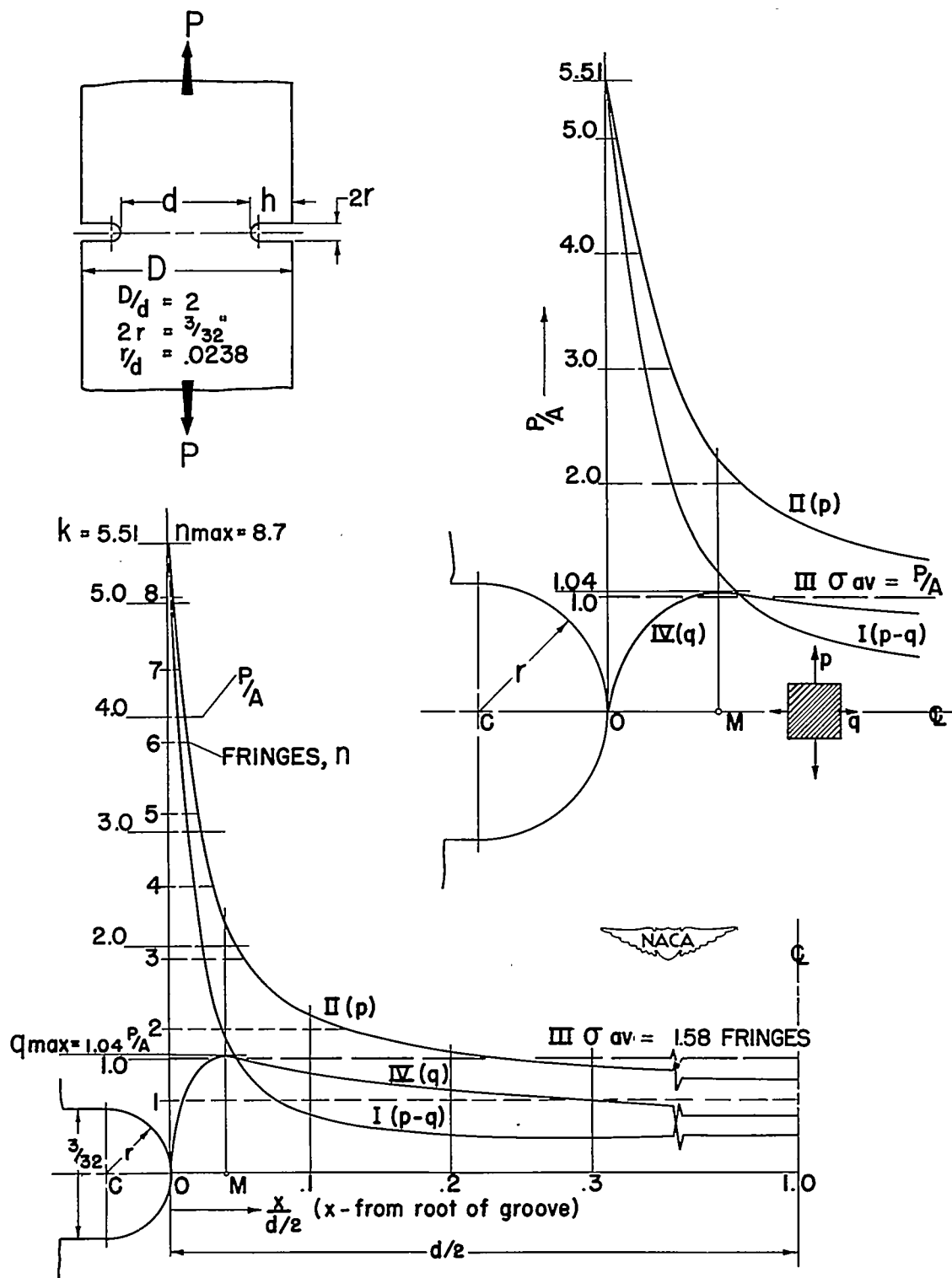
(c) Model C; $D/d = 1.5$; $r/d = 0.0334$; $2r = 3/16$ inch.

Figure 8.- Concluded.



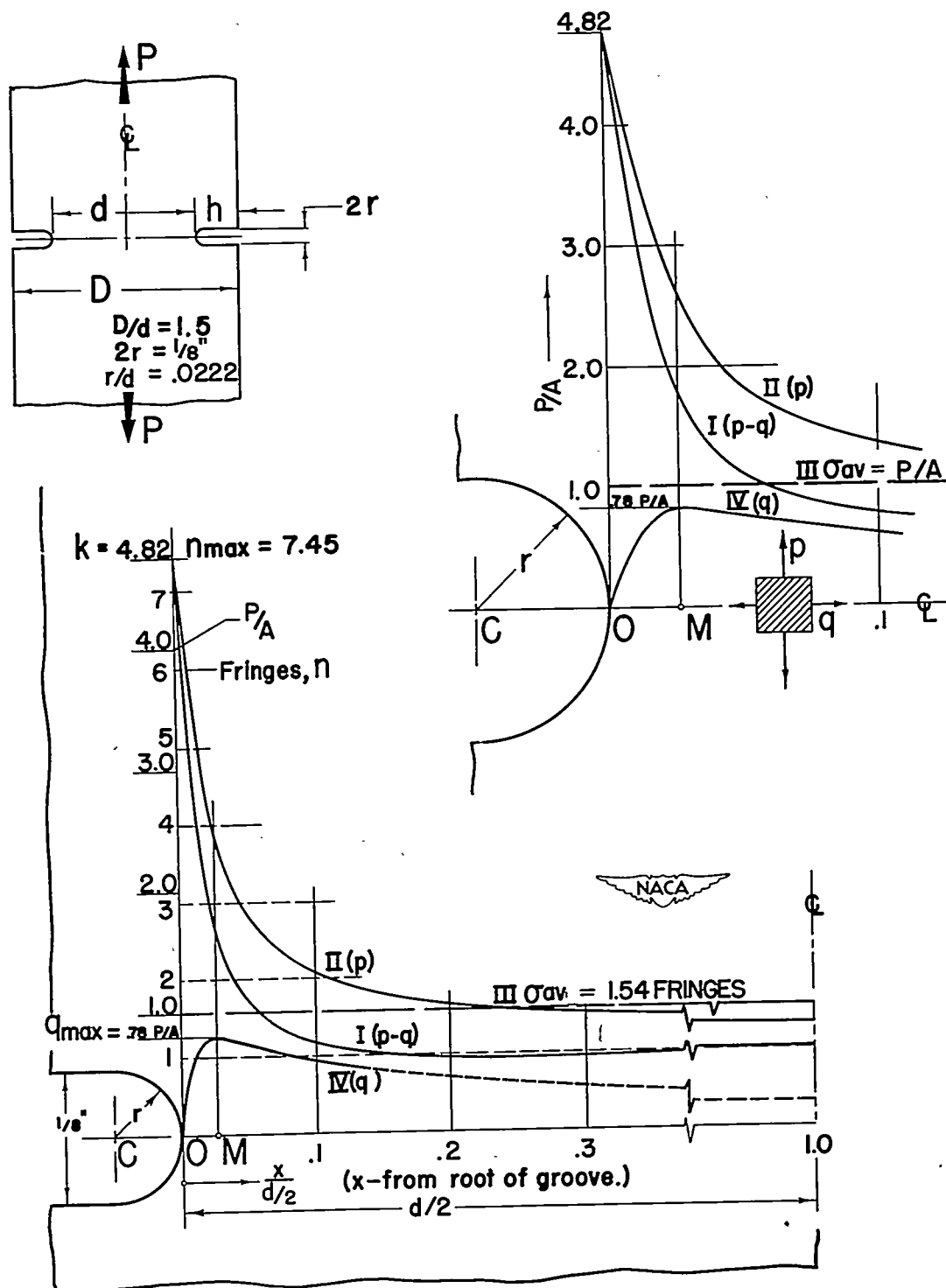
(a) Model F; $D/d = 2.0$; $r/d = 0.0159$; $2r = 1/16$ inch.

Figure 9.- Distribution of principal stresses p and q for section through grooves obtained by using values of $p + q$ from isopachic patterns.



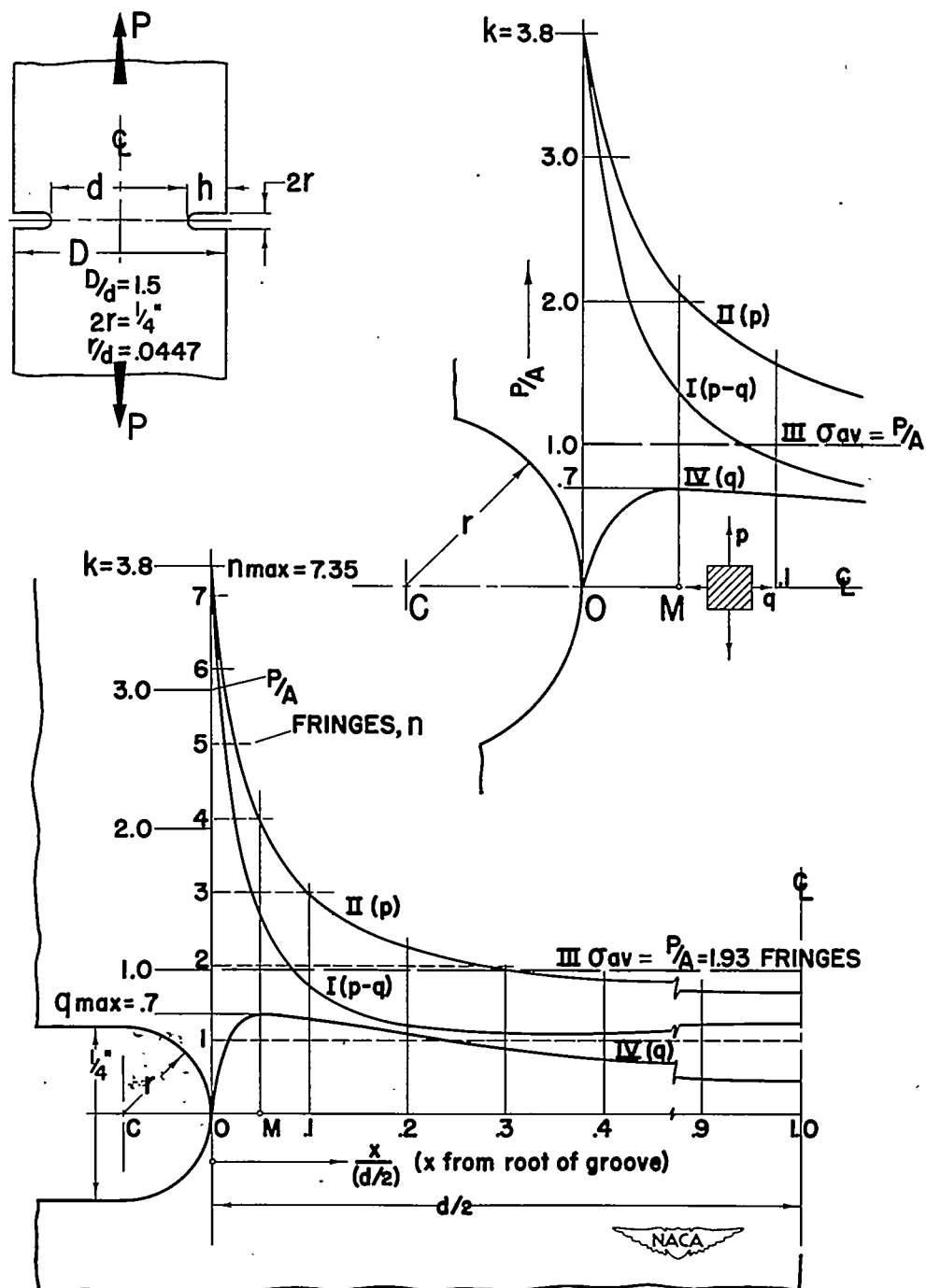
(b) Model F; $D/d = 2.0$; $r/d = 0.0238$; $2r = 3/32$ inch.

Figure 9.- Continued.



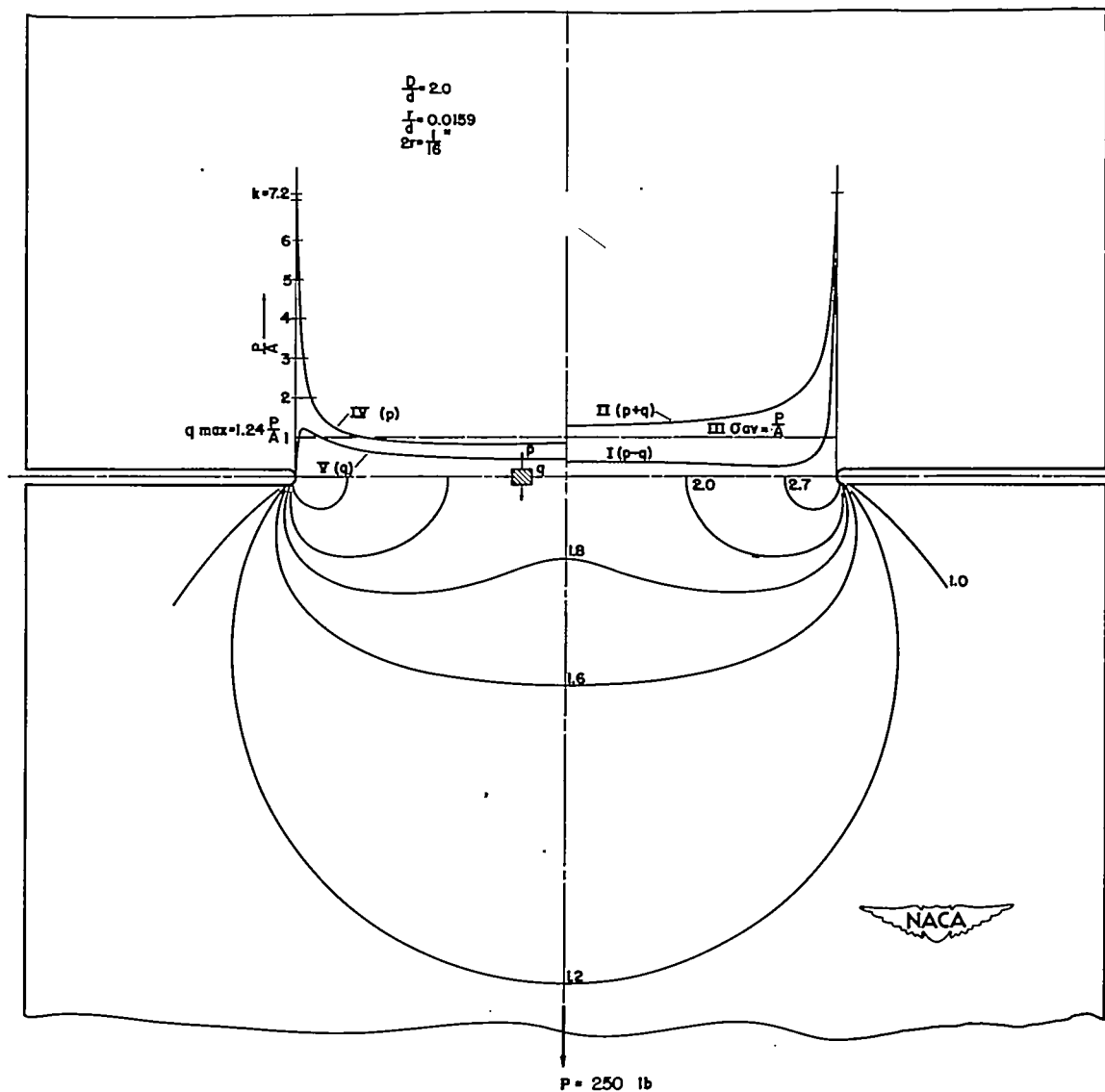
(c) Model C; $D/d = 1.5$; $r/d = 0.0222$; $2r = 1/8$ inch.

Figure 9.- Continued.



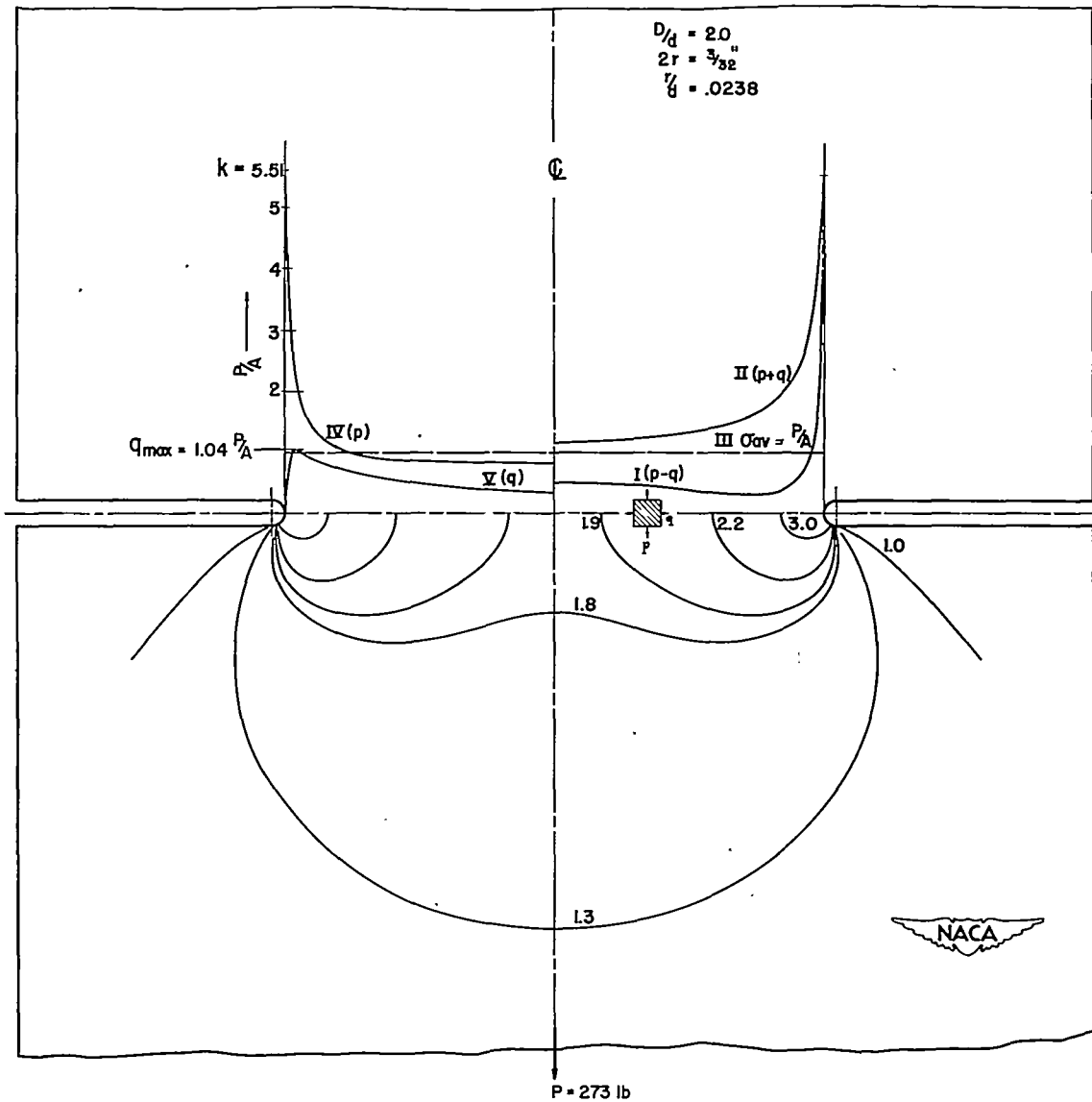
(d) Model C; $D/d = 1.5$; $r/d = 0.0447$; $2r = 1/4$ inch.

Figure 9.- Concluded.



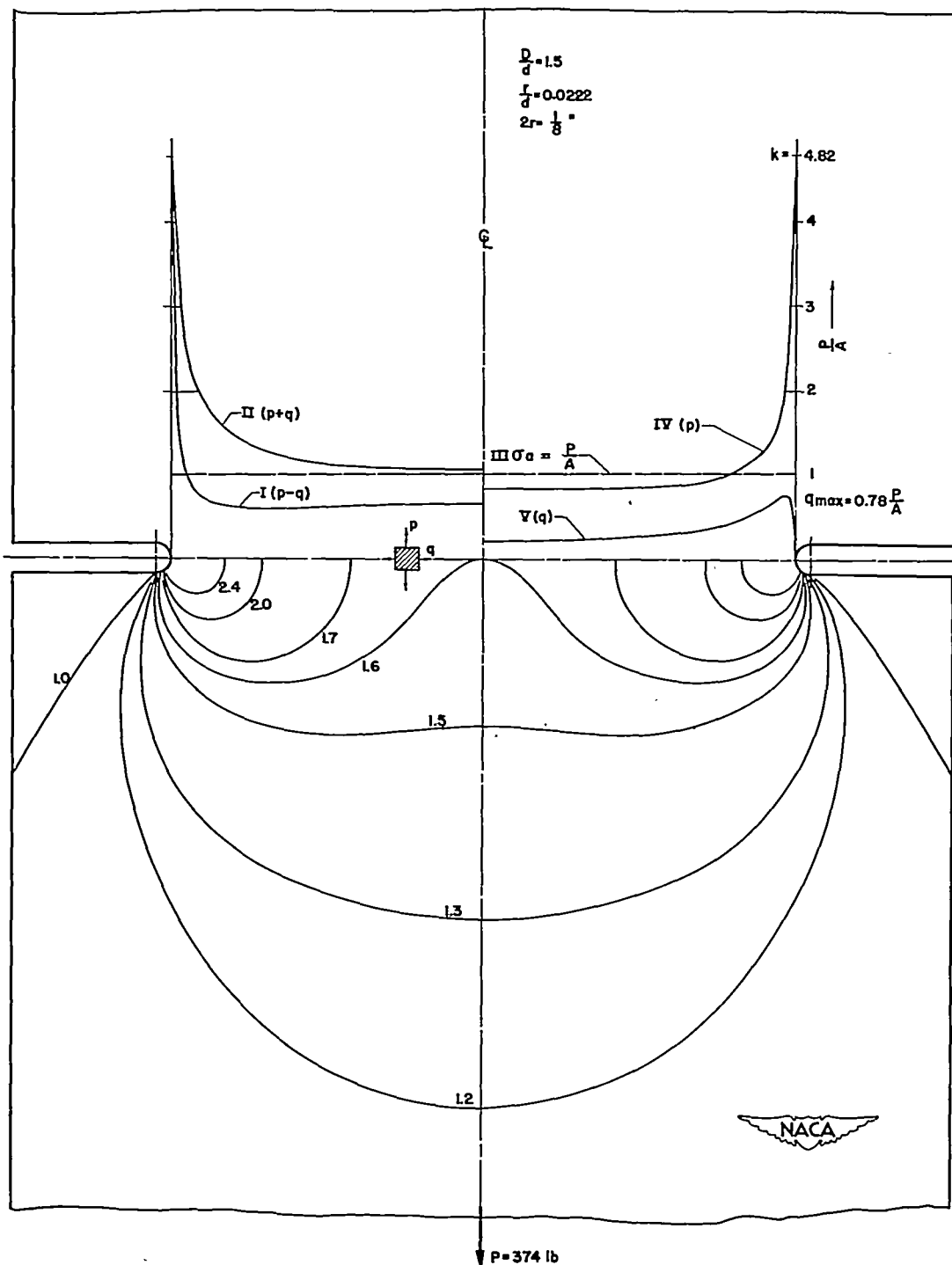
(a) Model F; $D/d = 2.0$; $r/d = 0.0159$; $2r = 1/16$ inch.

Figure 10.- Isopachic pattern and distribution of p and q across section through grooves obtained from numerical solution of Laplace's equation.



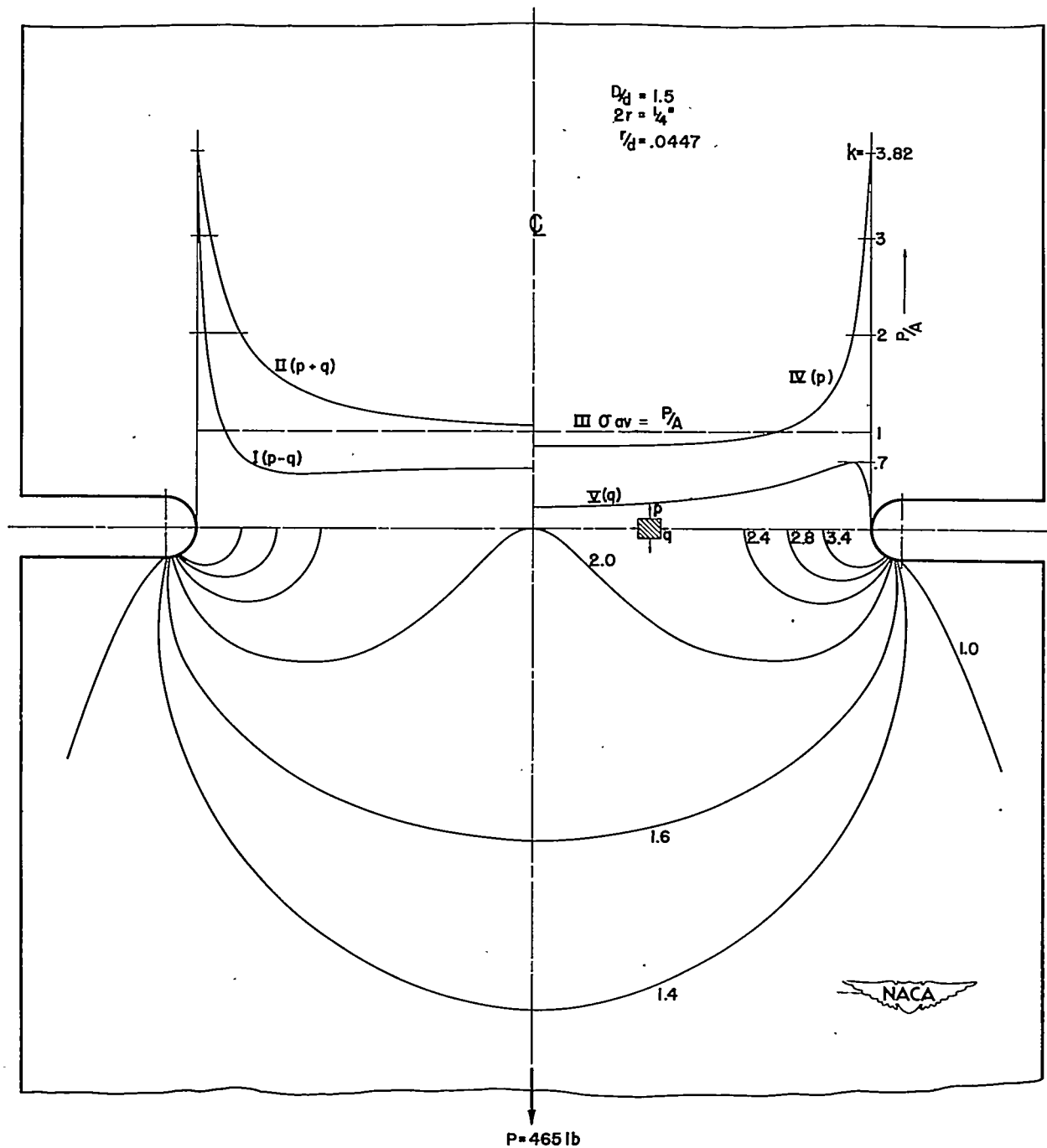
(b) Model F; $D/d = 2.0$; $r/d = 0.0238$; $2r = 3/32 \text{ inch}$.

Figure 10.- Continued.



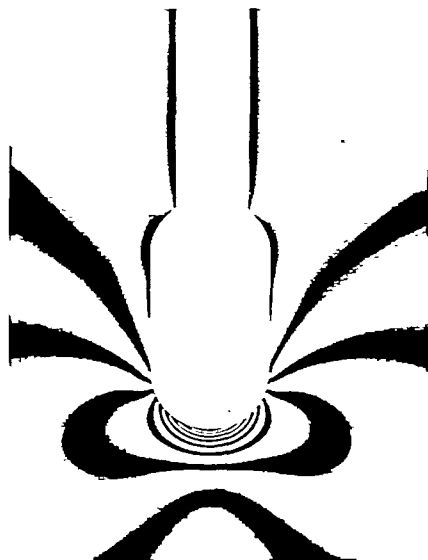
(c) Model C; $D/d = 1.5$; $r/d = 0.0222$; $2r = 1/8$ inch.

Figure 10.- Continued.

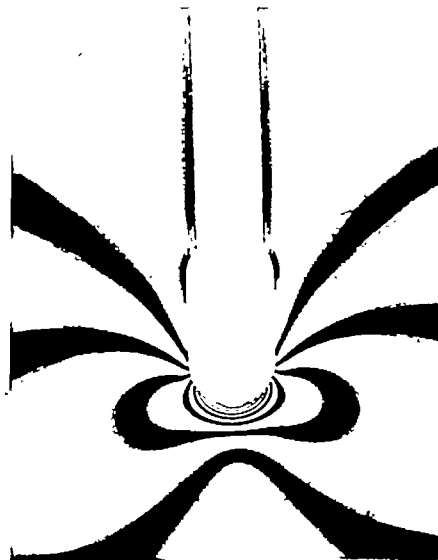


(d) Model C; $D/d = 1.5$; $r/d = 0.0447$; $2r = 1/4$ inch.

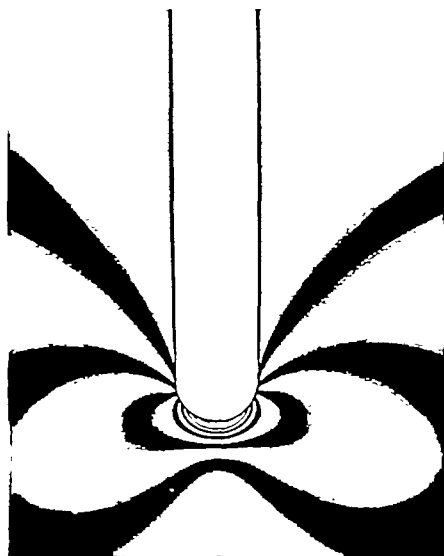
Figure 10.- Concluded.



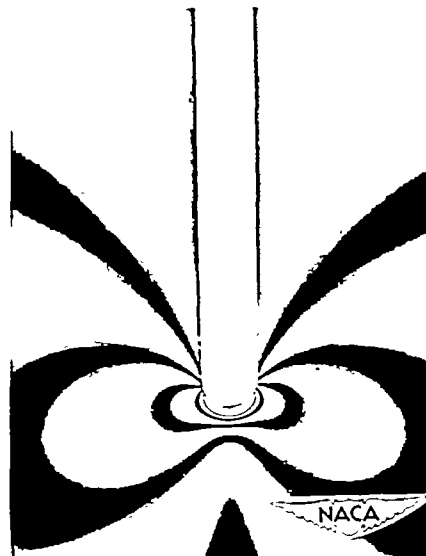
(a) $r/d = 0.0397$; $2r = 5/32$ inch;
 $P = 360$ pounds; $\sigma_{av} = 1220$ psi.
 Groove modified to reduce time of
 machining; modification does not
 affect values of k .



(b) $r/d = 0.0318$; $2r = 1/8$ inch;
 $P = 344$ pounds; $\sigma_{av} = 1167$ psi.
 Groove modified to reduce time of
 machining; modification does not
 affect values of k .

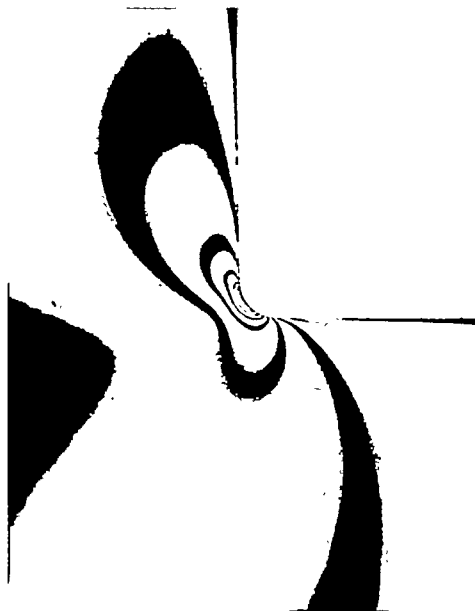


(c) $r/d = 0.0238$; $2r = 3/32$ inch;
 $P = 273$ pounds; $\sigma_{av} = 925$ psi.

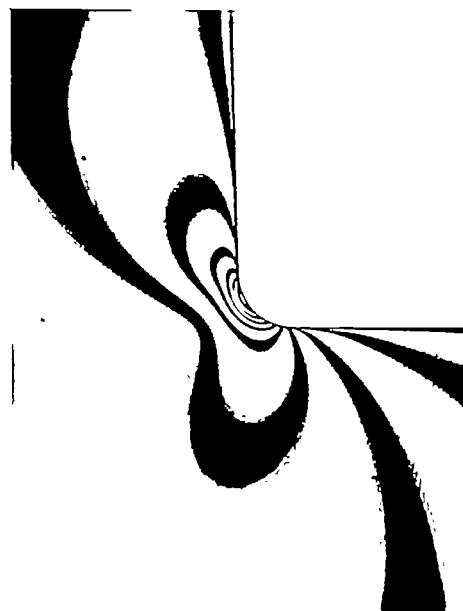


(d) $r/d = 0.0159$; $2r = 1/16$ inch;
 $P = 250$ pounds; $\sigma_{av} = 845$ psi.

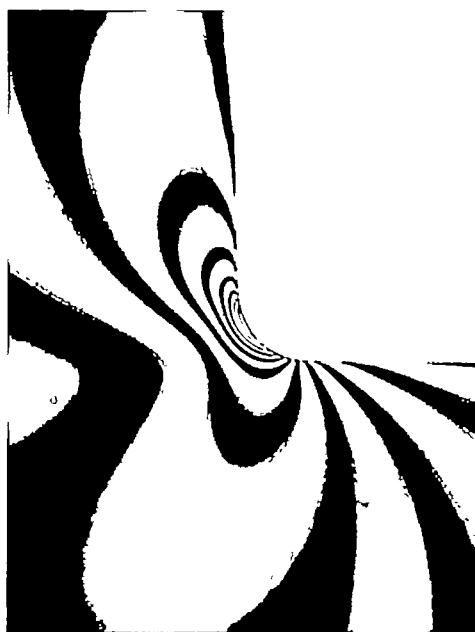
Figure 11.- Typical stress patterns of grooves from model F. Tensile loads in horizontal direction. $D = 3.879$ to 3.937 inches; nominal $D/d = 2.00$; $L = 10\frac{3}{4}$ inches; $t = 0.150$ inch; $F = 585$ psi tension.



(a) $r/d = 0.0164$; $2r = 1/16$ inch;
 $P = 323$ pounds; $\sigma_{av} = 1130$ psi.



(b) $r/d = 0.0246$; $2r = 3/32$ inch;
 $P = 379$ pounds; $\sigma_{av} = 1320$ psi.

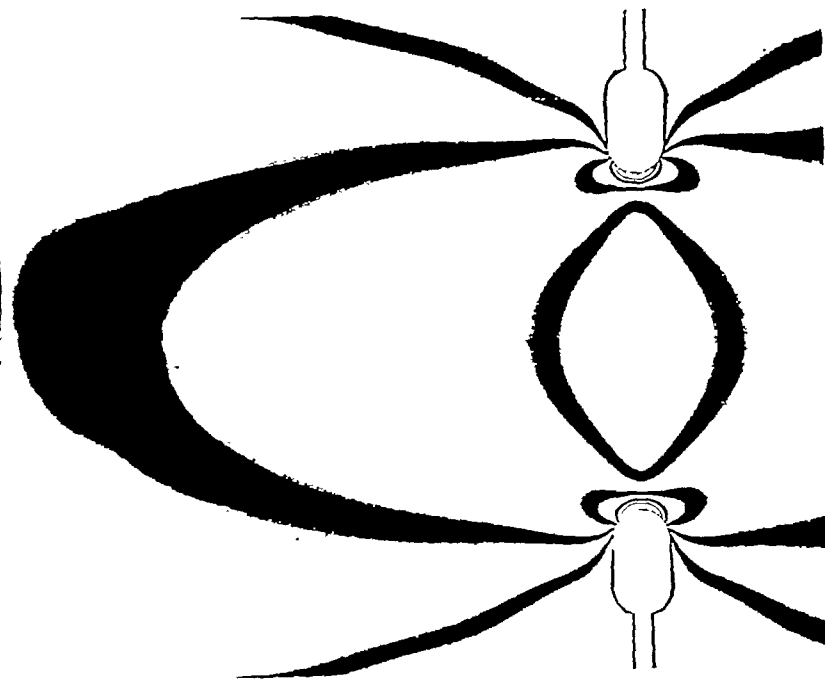


(c) $r/d = 0.0328$; $2r = 1/8$ inch;
 $P = 544$ pounds; $\sigma_{av} = 1900$ psi.

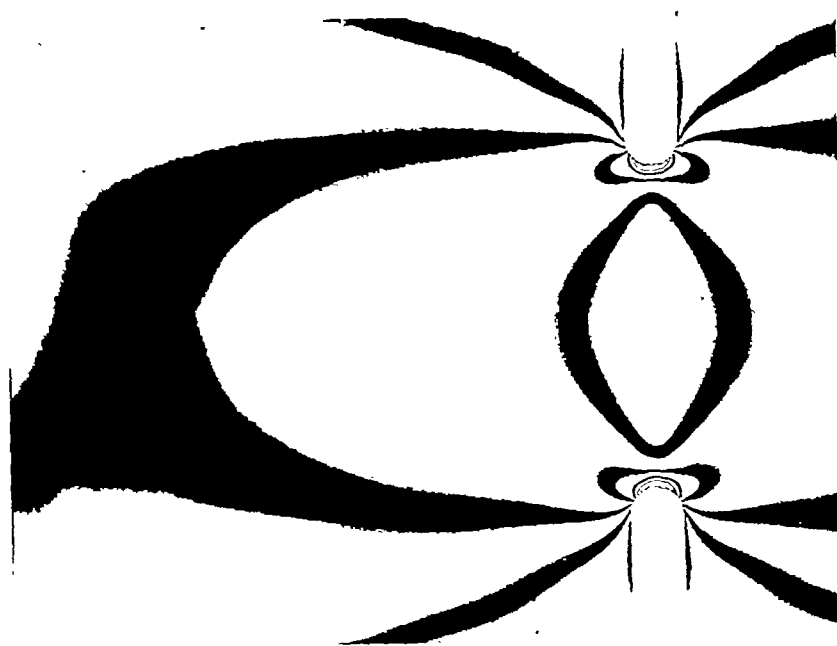


(d) $r/d = 0.0491$; $2r = 3/16$ inch;
 $P = 635$ pounds; $\sigma_{av} = 2210$ psi.

Figure 12.- Typical stress patterns of fillets from model G. Tensile loads in vertical direction. $D = 3.822$ inches; nominal $D/d = 2.00$; $L = 10\frac{3}{4}$ inches; $t = 0.150$ inch; $F = 585$ psi tension.



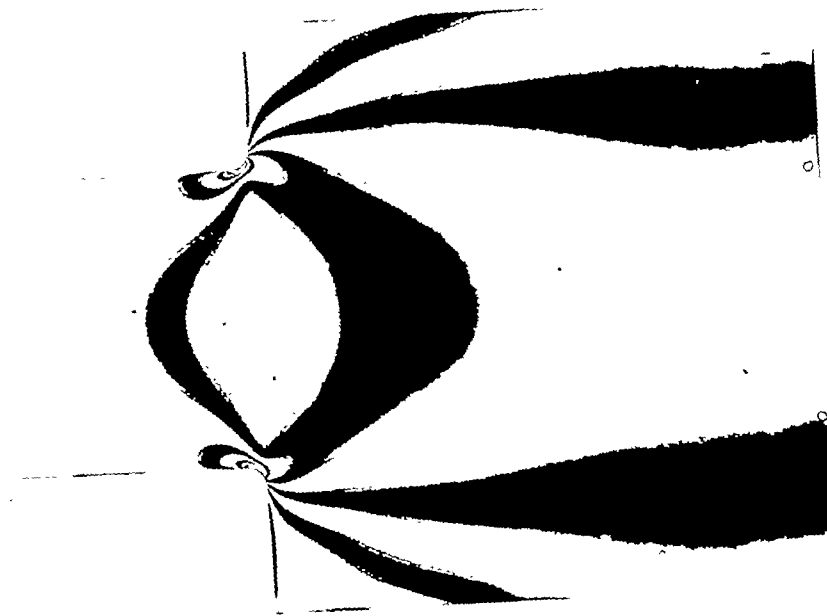
(a) Model F; modified grooves.



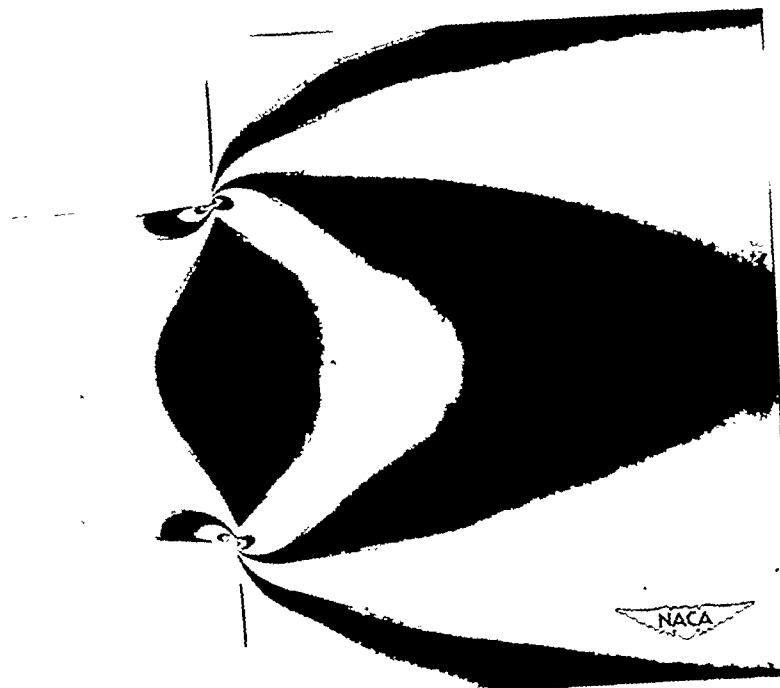
(b) Model F; straight grooves.



Figure 13.- Stress patterns of bars with grooves showing that modification of grooves has no effect on k . Tensile loads in horizontal direction. $r/d = 0.0805$; $2r = 5/16$ inch; $P = 413$ pounds; $\sigma_{av} = 1430$ psi; $D = 3.879$ inches; nominal $D/d = 2.00$; $L = 10\frac{3}{4}$ inches; $t = 0.150$ inch; $F = 585$ psi tension.



(a) Model G; $r/d = 0.0655$; $2r = 1/4$ inch; $P = 665$ pounds; $\sigma_{av} = 2310$ psi.



(b) Model G; $r/d = 0.0164$; $2r = 1/16$ inch; $P = 342$ pounds; $\sigma_{av} = 1190$ psi.

Figure 14.- Stress patterns of bars with fillets. Tensile loads in horizontal direction. $D = 3.822$ inches; $D/d = 2.00$; $L = 10\frac{3}{4}$ inches; $t = 0.150$ inch; $F = 585$ psi tension.

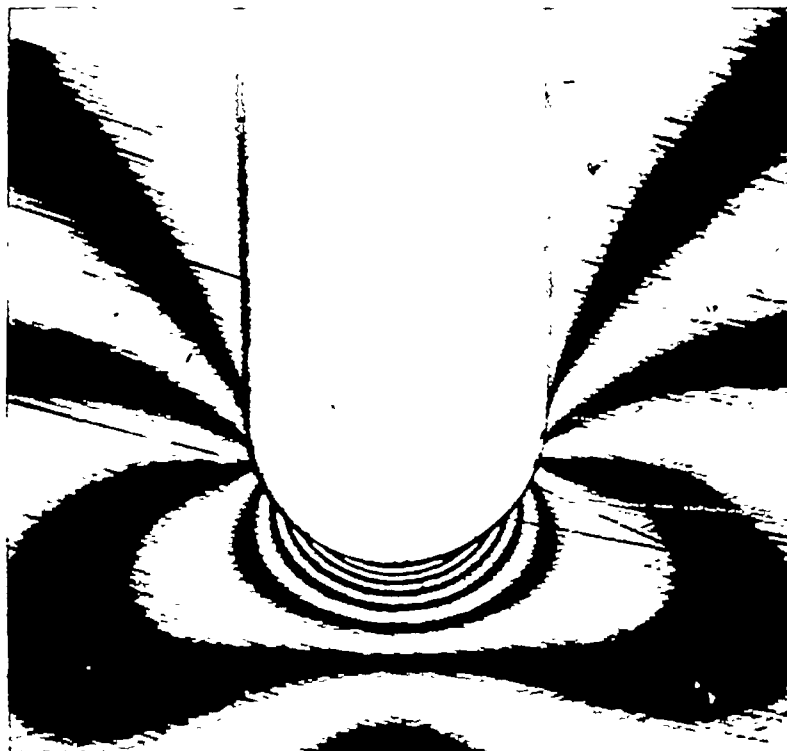


Figure 15.- Stress pattern for bar with grooves; distance between last two fringes is less than 0.002 inch. Model H; $r/d = 0.0268$; $2/r = 1/16$ inch; $P = 189$ pounds; $\sigma_{av} = 1910$ psi; $D = 1.745$ inches; nominal $D/d = 1.50$; $L = 10\frac{1}{8}$ inches; $t = 0.085$ inch; $F = 1015$ psi tension.

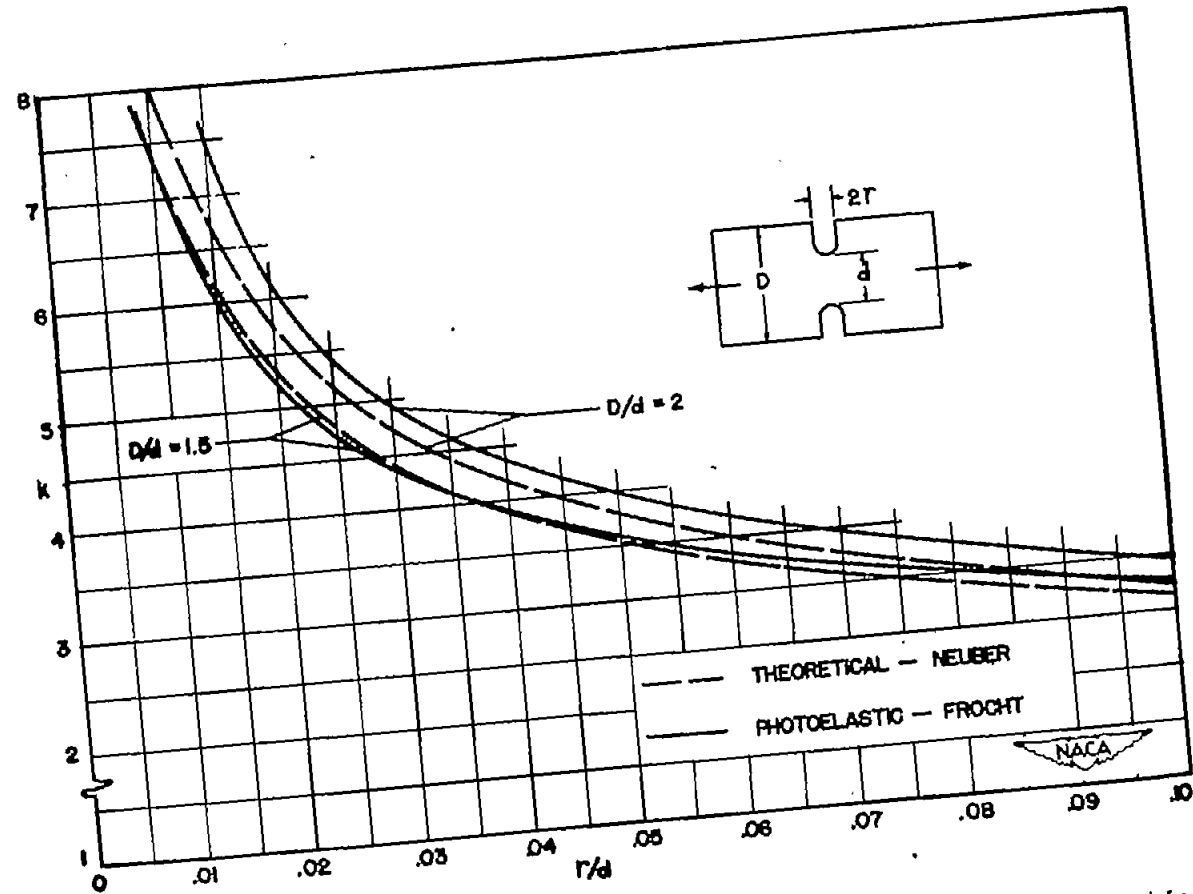


Figure 16.- Comparison of theoretical (reference 3) and photoelastic values of k for deep grooves in tension.